

Supporting information

N-heterocyclic Carbene(Cu) Synergistic Photothermal Hydrogen Release Involving Double Hydrogen Transfer Catalyzed by Porphyrin(Cu)-Based Conjugated Microporous Polymers for Efficient Quinoline Hydrogenation

*Lingjuan Zhang,^{*a} Jiayi Zheng,^a Nan Zhang,^a Jincong Yuan,^a Xian-Ming Zhang^{* a,b}*

Table of Contents

Section 1. Chemicals and Instrumentation.....	S2
Section 2. The preparation of monomers and ploymers	S4
Section 3. The characterization of ploymers.....	S7
Section 4. Catalysis	S15
Section 5. NMR, GC-MS data of products.....	S17
Section 6. NMR spectra of products.....	S23
Section 7. References.....	S41

Section 1. Chemicals and Instrumentation.

Unless otherwise stated, all chemicals are purchased from commercial sources and can be used without further purification. The water used in all experiments is deionized water.

Fourier transform infrared (FT-IR) spectra were obtained using FTIR-650 spectrometer (frequency range from 4000 to 400 cm^{-1}) with KBr pellet. The PXRD pattern was measured with a Cu target tube at 40 kV and 30 mA on Rigaku MiniFlex 600 diffractometer. The morphology analysis of the as-prepared samples were conducted on a scanning electron microscope (SEM, S4800, Hitachi Co., Japan). The UV-vis spectra of the samples were measured on a TU-1901 Ultraviolet spectrometer at room temperature and BaSO_4 was used as the reflectance standard reference. X-ray photoelectron spectroscopy (XPS) was performed on Thermo SCIENTIFIC™ ESCALAB 250Xi spectrometer with K-Alpha+ X-ray source. Energy (BE) is calibrated by setting the measured BE of C 1s to 284.8 eV. Thermo gravimetric analysis (TGA) was carried out on Shanghai Yinnuo 1000 B in N_2 atmosphere at a heating rate of 10 $^\circ\text{C min}^{-1}$. $^1\text{H-NMR}$, $^{13}\text{C-NMR}$ data were recorded on Bruker Avance III DM 600 MHz. Solid-state $^{13}\text{C CP-MAS}$ NMR spectra were conducted on a Bruker Avance-600 spectrometer. GC-MS analyses were obtained on a Shimadzu QP-2020. The adsorption-desorption isotherms of N_2 were measured at 77 K using ASPS 2020 gas sorption analyzer. Inductively coupled plasma (ICP) analysis was performed on a PerkinElmer Optima 8000 ICP-OES instrument. High resolution mass spectra data were recorded on Bruker IMPACT II. Photoluminescence spectra and fluorescence lifetimes test were conducted on Edinburgh FLS920 Fluorescence Spectrometer.

All products were isolated by flash column chromatography on silica gel with petroleum ether/ethyl acetate as eluents. Products are known compounds and are characterized by comparison of their $^1\text{H NMR}$, $^{13}\text{C NMR}$ spectra data and mass data with those reported in the literatures. All chemical shifts (δ) were reported in ppm and coupling constants (J) in Hz. All chemical shifts were reported relative to tetramethylsilane (0 ppm for ^1H) and CDCl_3 (77.16 ppm for ^{13}C), respectively.

Electrochemical measurements: the photoelectrochemical measurements were carried out in CHI-660 electrochemical station (Chenhua instrument, Shanghai, China) using a common three electrode configuration with Pt foil as the counter electrode and Ag/AgCl (saturated KCl) as the reference electrode. Na_2SO_4 (0.2 M) solution was used as the electrolyte and Xe lamp (300W, $\lambda \geq 420 \text{ nm}$, CEL-HXE 300, Beijing China Education Au-light Technology Co., Ltd). The working electrodes were prepared by the

following steps: 5 mg of photocatalyst was well dispersed in 0.5 mL ethanol containing 10 μ L nafion and sonicated for 10 min. Next, 250 μ L above suspension was dispersed dropwise onto the surface of a clear ITO glass with exposed 1×1 cm² area. After drying overnight in oven, the loading mass was about 0.4 mg/cm². The photocurrent response was measured at + 0.4 V bias voltage under chopped light and the Mott-Schottky plots were tested in the dark at 300/500/1000 Hz. The electrochemical impedance spectroscopy (EIS) measurement was performed in the frequency range from 10⁻² to 10⁶ Hz with a bias potential of 0.4 V.

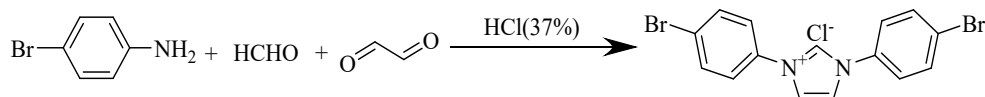
Cyclic voltammetry (CV) experiments were measured on a CHI 660E in a three-electrode electrochemical cell and a scan rate of 50 mV s⁻¹. The experiments were conducted in anhydrous acetonitrile with tetrabutylammonium hexafluorophosphate (0.1 M) as supporting electrolyte. The reference electrode was based on the Ag/Ag⁺ couple. The working electrode was a glassy carbon electrode. The auxiliary electrode was a platinum flakelet.

All computational studies were conducted using the Gaussian 16 software package^[1]. The DFT calculations were performed with the Becke's three-parameter hybrid method with the Lee, Yang, and Parr (B3LYP) gradient-corrected correlation functional.^[2] The all-electron basis set 6-31+G(d,p) was adopted for all atoms.

Section 2. The preparation of monomers and polymers.

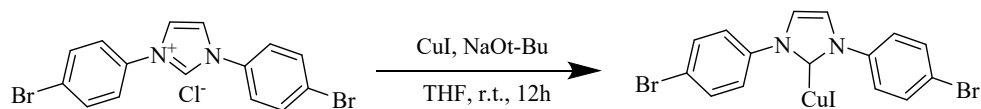
1. Monomer Synthesis

1.1 Synthesis of 1,3-bis(4-bromophenyl)-1H-imidazol-3-ium chloride (**Im**)³

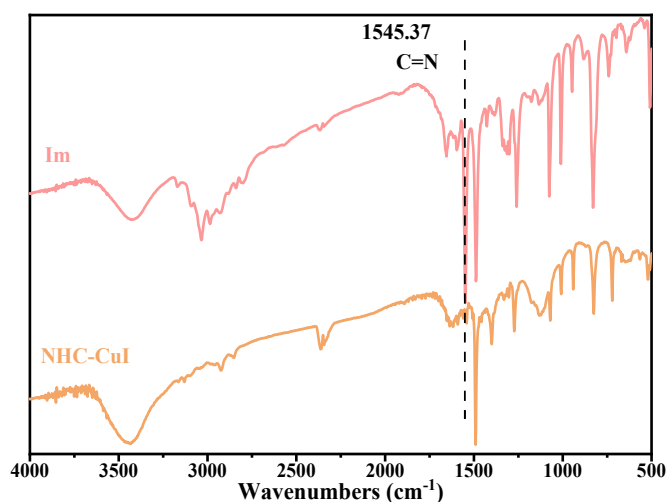


Formaldehyde polymer (98 mg, 3.3 mmol) was introduced into a 50 mL round-bottom flask, followed by the addition of 10 mL of toluene. A mixture of p-bromoaniline (1.0 g, 6.0 mmol) and a 40% (v/v) aqueous solution of glyoxal (4.0 g, 3.0 mmol) in 5 mL of toluene was prepared separately and then slowly added to the reaction mixture. Subsequently, HCl [37% (v/v), 0.3 mL, 3 mmol] was added dropwise to the above mixture. The reaction mixture was refluxed at 140°C using a Dean-Stark apparatus until no further increase in collected water volume was observed. The solvent was removed under reduced pressure by rotary evaporation, and the residue was dissolved in acetonitrile followed by filtration to remove insoluble impurities. After removal of the solvent by rotary evaporation, a light brown powder was obtained. The product was subsequently characterized by ¹H NMR spectroscopy.

1.2 Synthesis of NHC(Cu)⁴

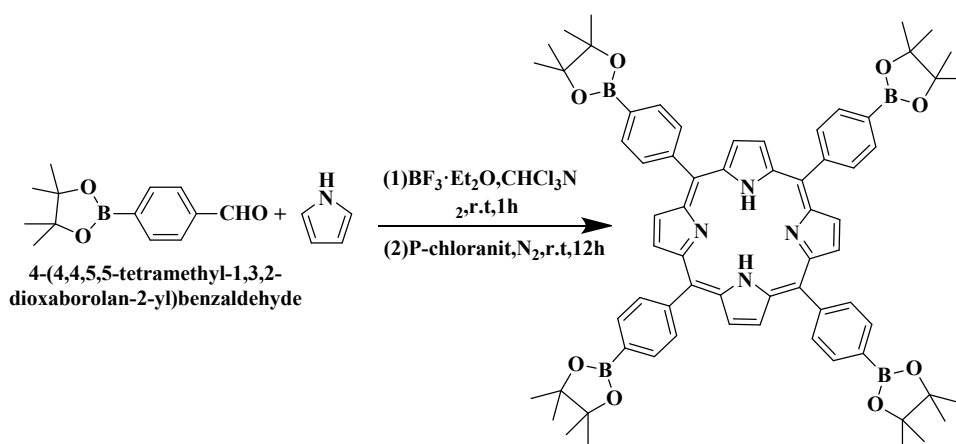


In a 50 mL round-bottom flask, the imidazole monomer **Im** (1.0 equiv, 0.04 mmol, 15 mg), sodium tert-butoxide (1.0 equiv, 0.08 mmol, 7.69 mg), and copper(I) iodide (1.0 equiv, 0.04 mmol, 7.6 mg) were added sequentially, followed by the addition of 2 mL of anhydrous tetrahydrofuran under inert atmosphere. The reaction was conducted under a nitrogen atmosphere at room temperature for 12 hours. Upon completion, 6 mL of deionized water was added, and the resulting mixture was stirred thoroughly to ensure complete phase separation. Centrifugation yielded a brown solid, which was subsequently washed with a mixed solvent system (isopropyl alcohol: petroleum ether = 1 : 3) until the filtrate became colorless. The product was then subjected to vacuum drying to afford the target carbene monomer, whose successful formation was confirmed by infrared spectroscopy.



1.3 Synthesis of 5,10,15,20-Tetrakis (4-boronic acid pinacol esterylphenyl) porphyrin (**Por**)^{5,6}

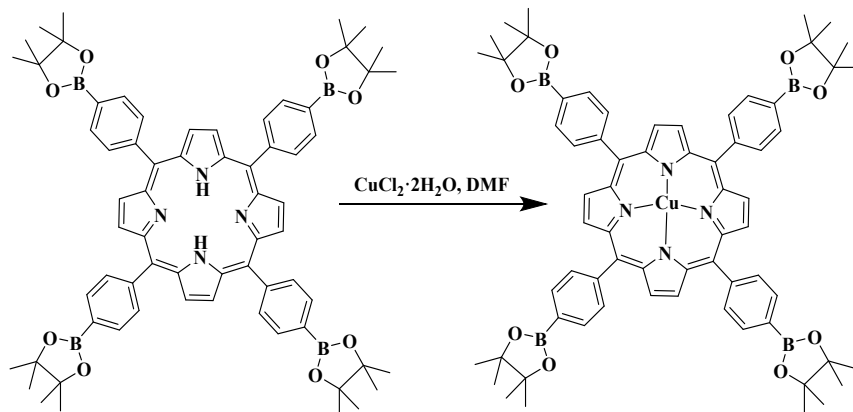
Referring to literature, the monomer **Por** was successfully synthesized. In a 500 mL flask, 4-(4,4,5,5-tetramethyl-1,3,2-dioxaboran-2-yl) benzaldehyde (0.232 g, 1 mmol) and pyrrole (0.07 mL, 1 mmol) were dissolved in 125 mL chloroform solvent, and the mixed solution was quickly frozen in a liquid nitrogen bath and filled with nitrogen. At room temperature, boron trifluoride ether complex ($\text{BF}_3 \cdot \text{Et}_2\text{O}$, 20 μL) was dissolved in 5 mL CHCl_3 and added to the system. After stirring for 1 h, tetrachlorobenzophenone (0.37 g, 1.5 mmol) was added to the reaction bottle in N_2 atmosphere. The reaction mixture was stirred at room temperature for 16 h. After rotational evaporation, the crude product was purified by column chromatography on silica gel to give as a purple powder.



1.4 Synthesis of **Por**(Cu)^{5,6}

Por (200 mg, 0.19 mmol) and $\text{CuCl}_2 \cdot 2\text{H}_2\text{O}$ (358 mg, 2.1 mmol) in 50 mL of DMF was refluxed for 16 h. When the mixture was cooled down to room temperature, H_2O was added until all solids are

precipitated. The mixture was filtered, the system was extracted with trichloromethane and saturated sodium chloride aqueous solution three times. The combined organic layer was dried over MgSO_4 and then evaporated to dryness to get red solid **Por(Cu)**.



2. Synthesis of **Im-PCMP**

A mixture of 1,3-bis(4-bromophenyl)-1H-imidazol-3-ium chloride (**Im**, 103.63 mg, 0.25 mmol), 5,10,15,20-Tetrakis (4-boronic acid pinacol esterylphenyl) porphyrin (**Por**, 139.83 mg, 0.125 mmol), tetrakis-(triphenylphosphine)palladium (0) (28 mg, 0.025 mmol), and K_2CO_3 (86.4 mg, 0.625 mmol) were degassed in a 50 mL flask. After that, a mixture solution of 28 mL N, N-dimethylformamide (DMF) and 2 mL H_2O was successively injected into the flask (**Scheme 1**, for details see the Supporting Information). The mixture solution was stirred at 100 °C for 3 days under a nitrogen atmosphere. After cooling to room temperature, the precipitate was centrifuged and washed three times with DMF, dichloromethane, methanol, and H_2O to remove unreacted monomer or residual catalysts, respectively. The black-purple powder was further purified by Soxhlet extraction from methanol and dichloromethane for 48 h. The obtained products were dried under vacuum at 80 °C for 12 h.

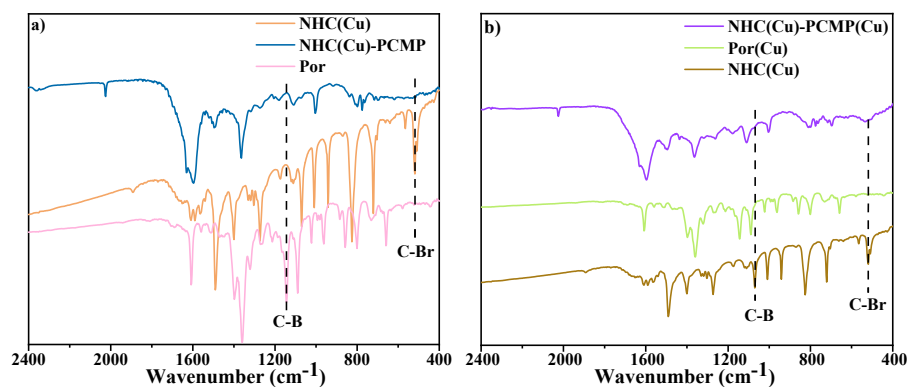
3. Synthesis of **NHC(Cu)-PCMP** and **NHC(Cu)-PCMP(Cu)**⁷

The synthesis method of **NHC(Cu)-PCMP** is similar to that of material **Im-PCMP**, simply replace the monomer **Im** with the monomer **NHC(Cu)** (142.38 mg, 0.25 mmol). The final product is brown powder in 58% isolation yield.

The synthesis method of **NHC(Cu)-PCMP(Cu)** is similar to that of material **NHC(Cu)-PCMP**, simply replace the monomer **Por** with the monomer **Por(Cu)** (147.52 mg, 0.125 mmol). The final product is dark brown powder in 60% isolation yield.

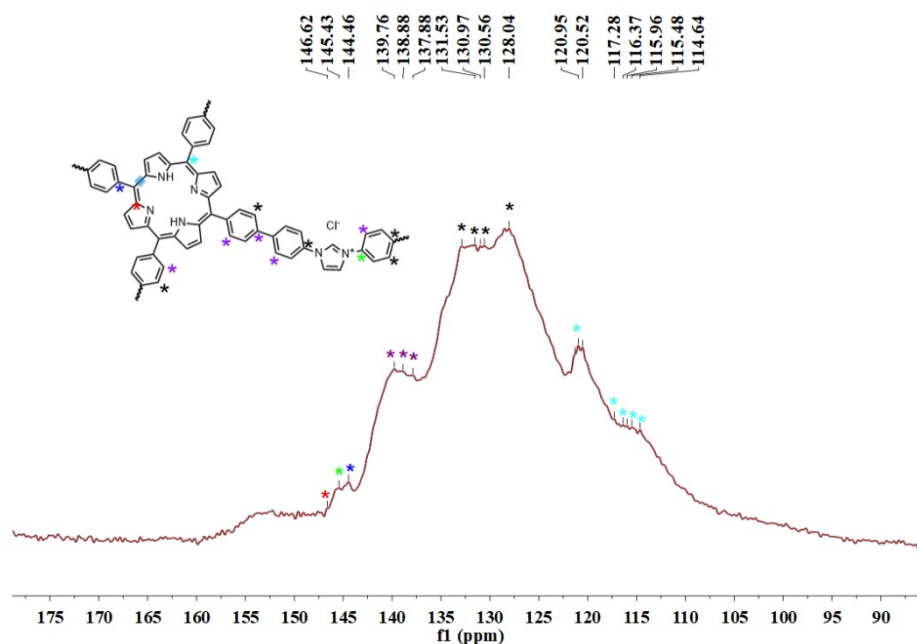
Section 3. The characterization of polymers.

1. FT-IR spectra of the monomers and NHC(Cu)-PCMP, NHC(Cu)-PCMP(Cu). (Figure. S1)

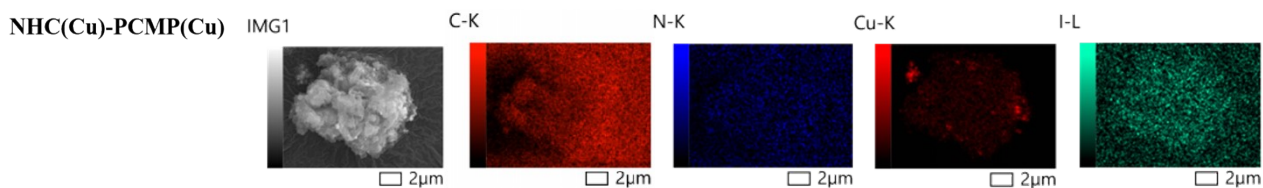


2. The solid-state ¹³C-MAS NMR spectrum of Im-PCMP. (Figure. S2)

a)



b)



Im-PCMP

Element	Line	Mass%	Atom%
C	K	74.30±0.03	78.82±0.03
N	K	21.69±0.10	19.73±0.09
Cl	K	4.01±0.01	1.44±0.00
Total		100.00	100.00
Map_003_wholespectrum		Fitting ratio 0.0970	

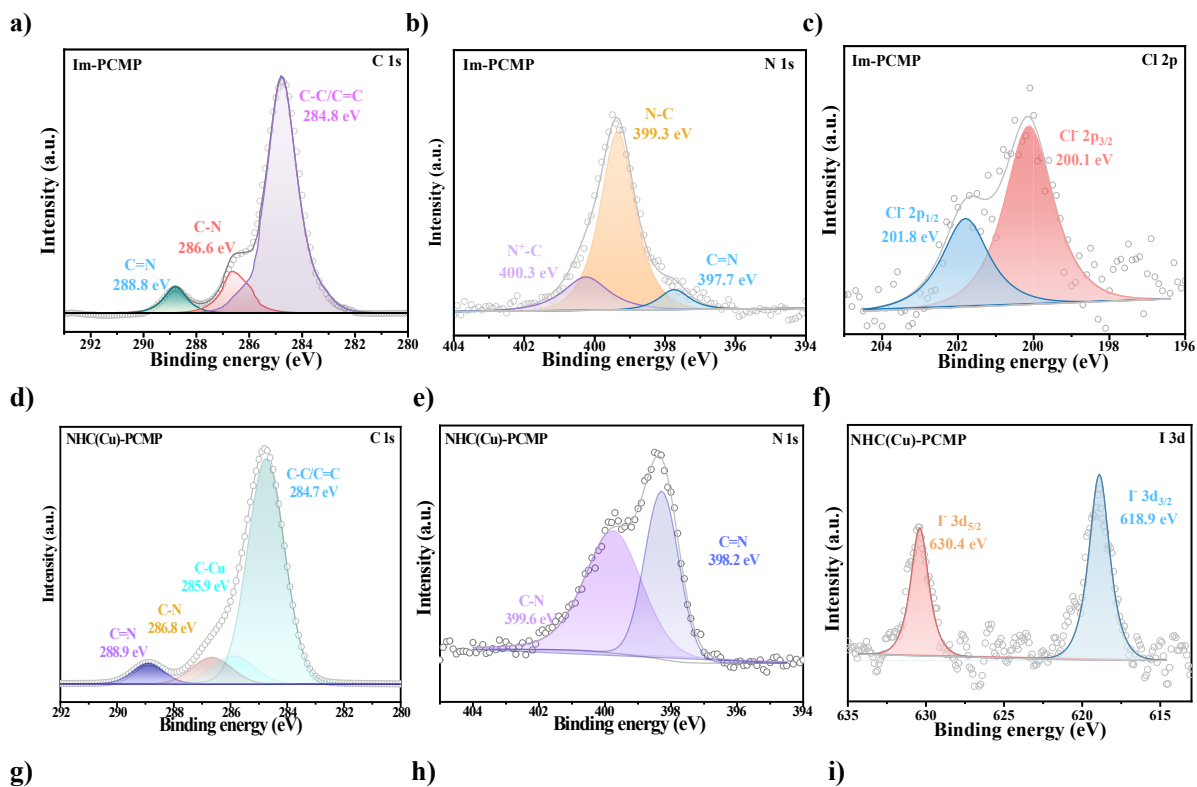
NHC(Cu)-PCMP

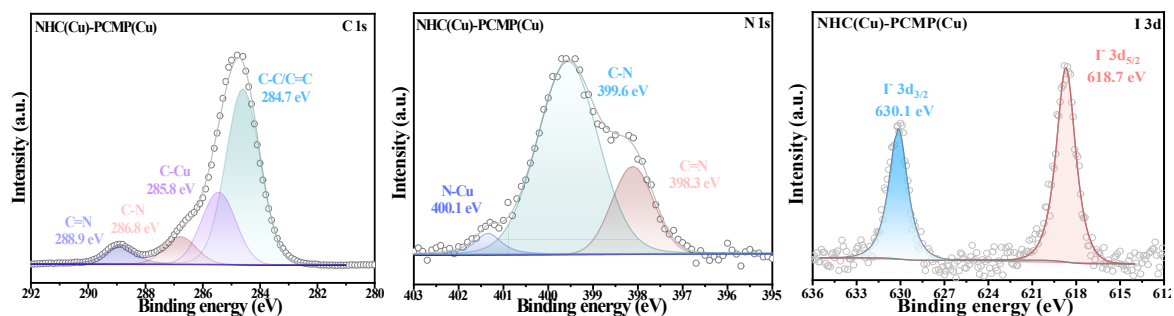
Element	Line	Mass%	Atom%
C	K	85.29±0.03	89.86±0.03
N	K	10.27±0.09	9.28±0.08
Cu	K	4.23±0.03	0.84±0.01
I	L	0.21±0.01	0.02±0.00
Total		100.00	100.00
Map_001_wholespectrum		Fitting ratio 0.0693	

NHC(Cu)-PCMP(Cu)

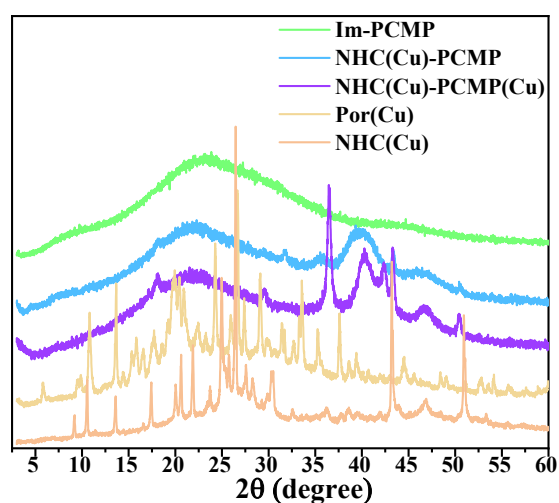
Element	Line	Mass%	Atom%
C	K	90.16±0.06	98.03±0.06
N	K	nd	nd
Cu	K	9.36±0.05	1.92±0.01
I	L	0.48±0.02	0.05±0.00
Total		100.00	100.00
Map_003_wholespectrum		Fitting ratio 0.3216	

4. The high-resolution XPS spectra of C 1s, N 1s, Cl 2p/I 3d of Im-PCMP, NHC(Cu)-PCMP and NHC(Cu)-PCMP(Cu); (Figure S4)

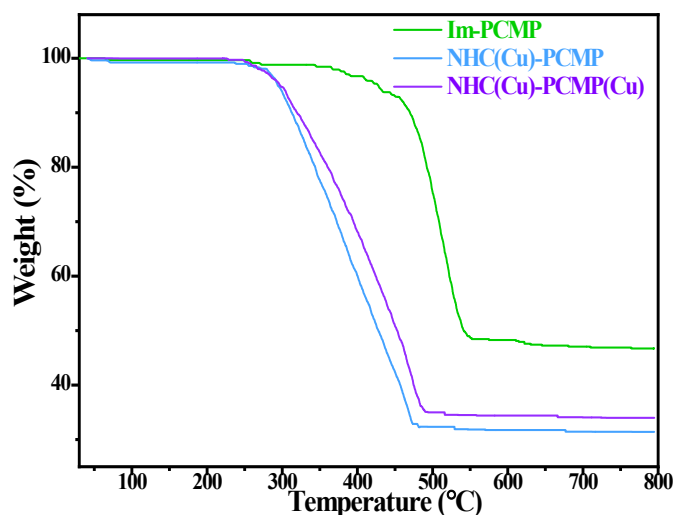




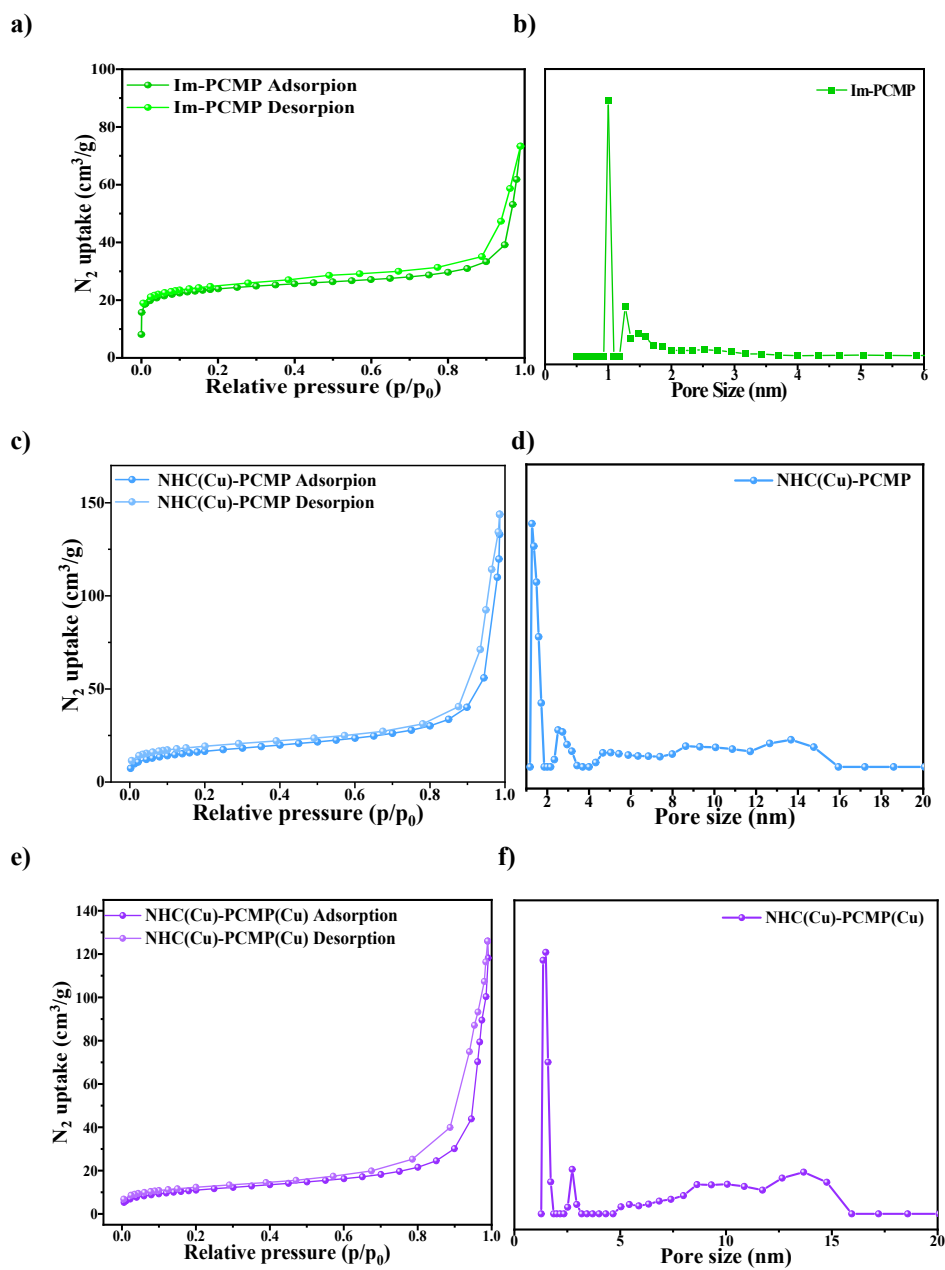
5. The PXRD spectra of Im-PCMP, NHC(Cu)-PCMP and NHC(Cu)-PCMP(Cu) samples and Por(Cu) and NHC(Cu). (Figure S5)



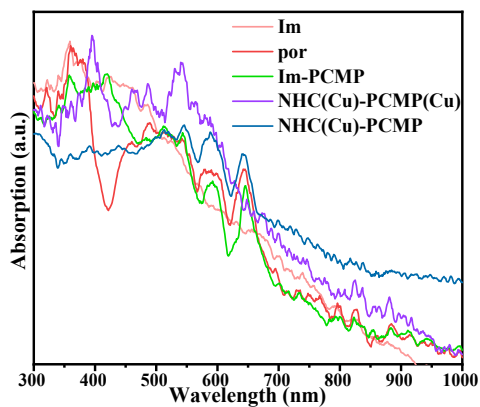
6. Thermogravimetric analysis curves of Im-PCMP, NHC(Cu)-PCMP and NHC(Cu)-PCMP(Cu) samples. (Figure S6)



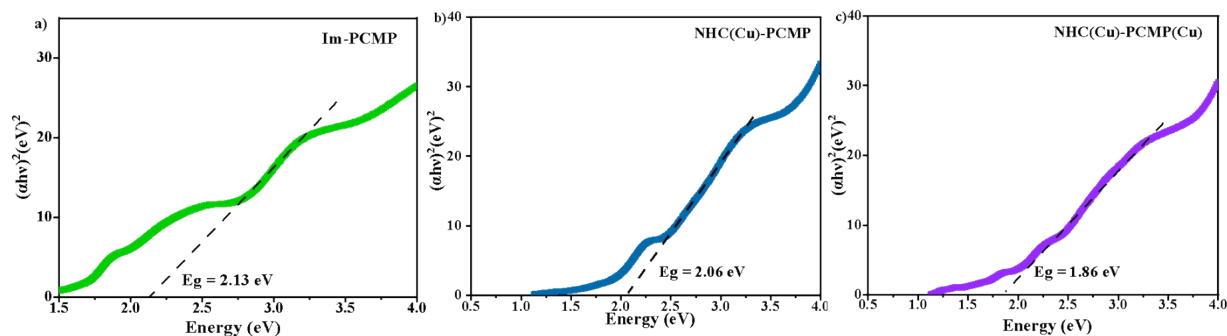
7. N₂ adsorption isotherms and pore size distributions Im-PCMP, NHC(Cu)-PCMP and NHC(Cu)-PCMP(Cu) samples. (Figure S7)



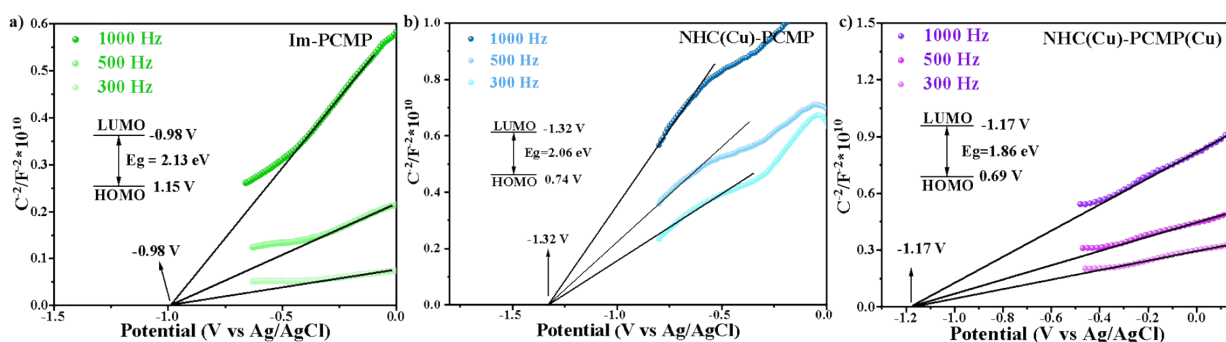
8. The UV-vis diffuse reflectance spectra of Im-PCMP, NHC(Cu)-PCMP and NHC(Cu)-PCMP(Cu) samples. (Figure S8)



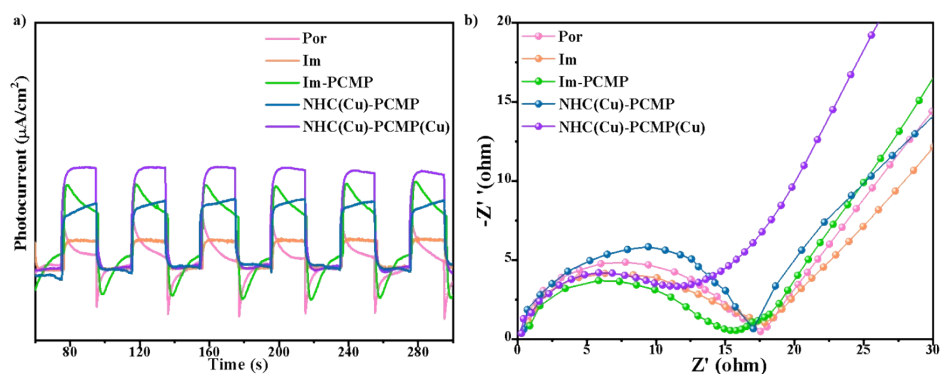
9. The corresponding tauc plots for the calculation of band gaps of a) Im-PCMP; b) NHC(Cu)-PCMP and c) NHC(Cu)-PCMP(Cu). (Figure S9)



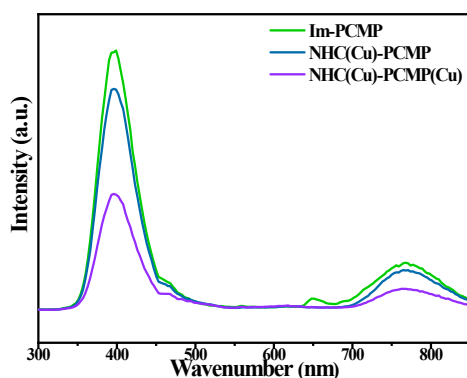
10. Mott-Schottky plot in 0.2 M Na₂SO₄ aqueous solution: a) Im-PCMP; b) NHC(Cu)-PCMP and c) NHC(Cu)-PCMP(Cu). (Figure S10)



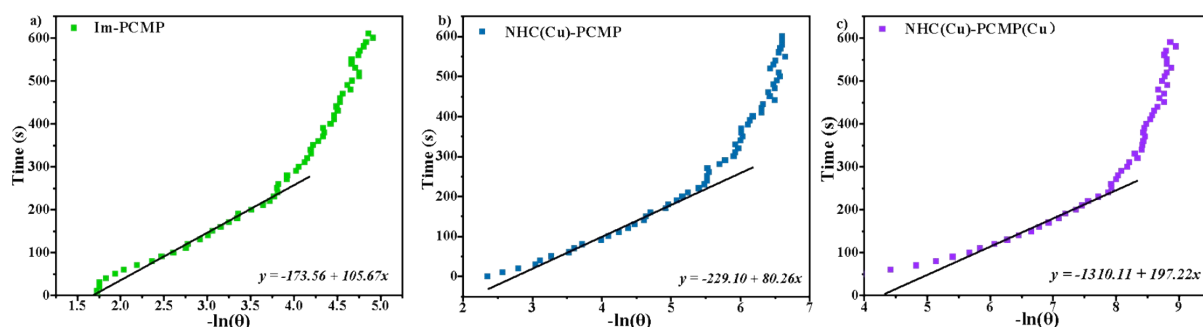
11. Transient photocurrent response and electrochemical impedance spectra of monomers and polymers. (Figure S11)



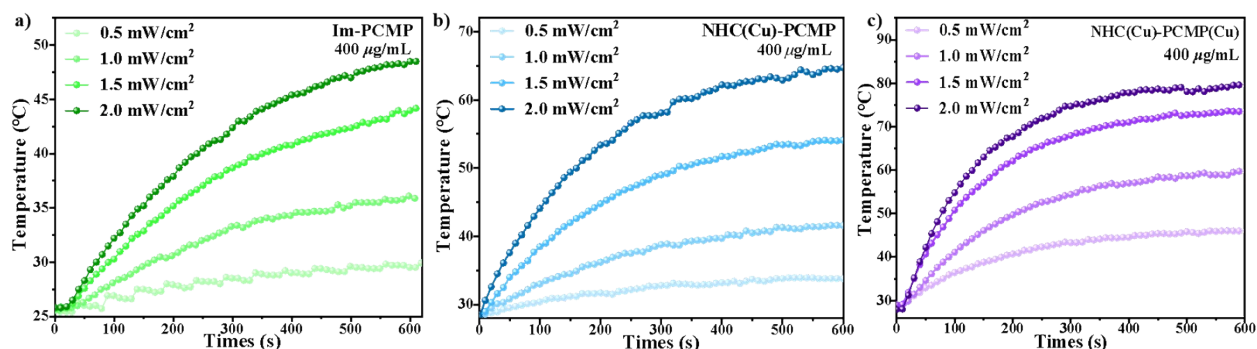
12. Photoluminescence spectra of Im-PCMP, NHC(Cu)-PCMP and NHC(Cu)-PCMP(Cu). (Figure S12)



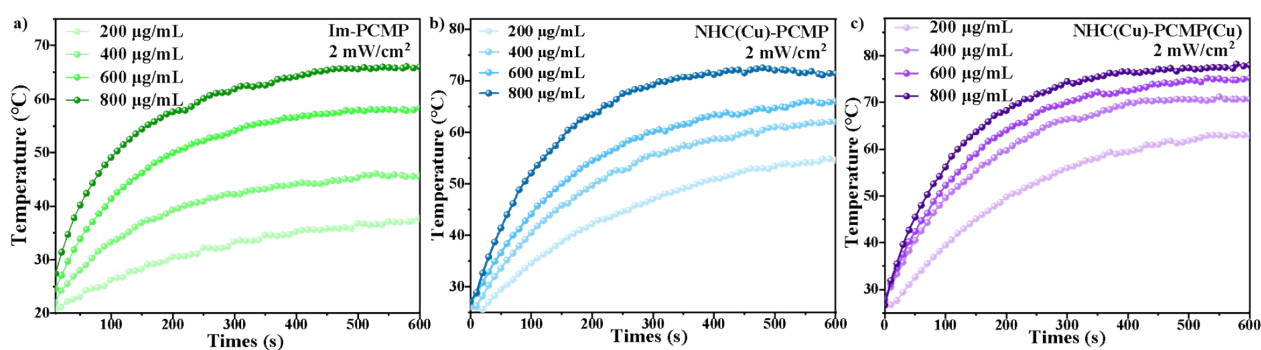
13. Linear fitting of Im-PCMP, NHC(Cu)-PCMP and NHC(Cu)-PCMP(Cu) to calculate the photothermal conversion efficiency. (Figure S13)



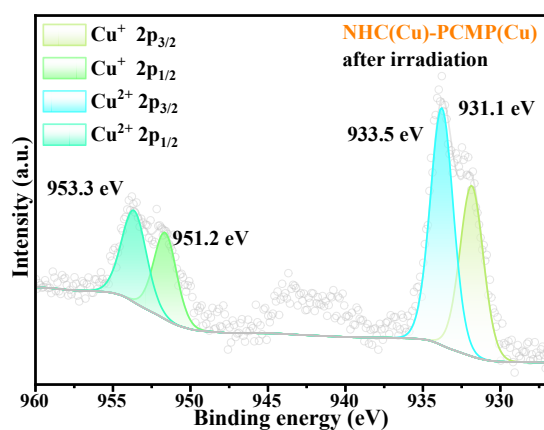
14. Temperature variation curves with different laser power densities under 808 nm laser irradiation ($400 \mu\text{g mL}^{-1}$). (Figure S14)



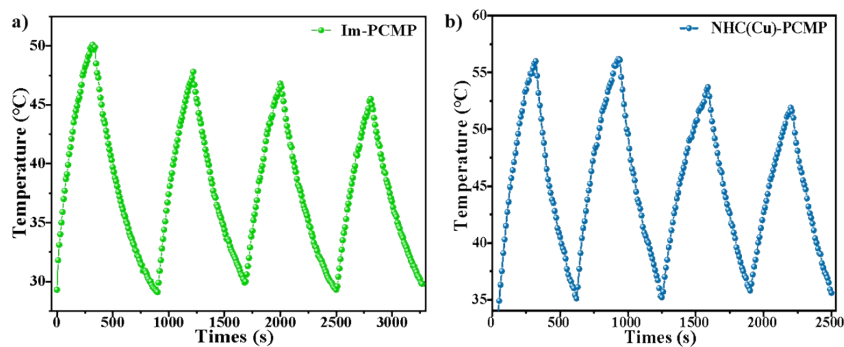
15. Temperature variation curves with different concentrations under 808 nm laser irradiation (2.0 W cm^{-2}). (Figure S15)



16. The Cu 2p XPS spectra of NHC(Cu)-PCMP(Cu) after irradiation. (Figure S16)



17. Laser on/off heating and cooling cycle of Im-PCMP, NHC(Cu)-PCMP for photostability tests (2.0 W cm⁻²). (Figure S17)



Section 4. Catalysis

1. Photocatalytic experiment

In a 5 mL branched Schlenk, **NHC(Cu)-PCMP(Cu)** (10 mg) was added in a mixture of toluene (1 mL), quinoline (**1a**, 0.2 mmol) and $t\text{-BuNH}_2\text{BH}_3$ (4eq., 0.8 mmol). The reaction was conducted under gentle stirring and irradiated with a 300 W Xe lamp ($\lambda \geq 420$ nm), while being monitored by GC-MS. Upon completion of the reaction, the catalyst was separated via centrifugation, extensively washed with methanol, and subsequently reused in further reaction cycles. The organic layers were quenched with 10 mL of saturated NaCl solution and subsequently extracted with dichloromethane (3×10 mL). The combined organic layers were concentrated under vacuum, and the residue was purified by flash column chromatography to afford product **2a**.

2. Condition optimization for transfer hydrogenation reaction of quinoline. (Table S1) ^{a,b}



Entry	Catalyst	Hydride [equiv.]	Sol.	Light	Time	Conv. [%]	Sel. [%]
1	NHC(Cu)-PCMP(Cu) (10 mg)	NH_3BH_3 (3)	toluene	Xe	12 h	12%	60%
2	NHC(Cu)-PCMP(Cu) (10mg)	$\text{PhEt}_2\text{NBH}_3$ (3)	toluene	Xe	12 h	32%	90%
3	NHC(Cu)-PCMP(Cu) (10 mg)	$t\text{BuNH}_2\text{BH}_3$ (3)	toluene	Xe	12 h	85%	100%
4	NHC(Cu)-PCMP(Cu) (10mg)	H_2 (1 atm)	toluene	Xe	5 h	-	-
5	NHC(Cu)-PCMP(Cu) (10mg)	$t\text{BuNH}_2\text{BH}_3$ (4)	toluene	Xe	5 h	94%	100%
6	NHC(Cu)-PCMP(Cu) (10mg)	$t\text{BuNH}_2\text{BH}_3$ (4)	EtOH	Xe	5 h	30%	100%
7	NHC(Cu)-PCMP(Cu) (10mg)	$t\text{BuNH}_2\text{BH}_3$ (4)	MeCN	Xe	5 h	41%	100%
8	NHC(Cu)-PCMP(Cu) (10mg)	$t\text{BuNH}_2\text{BH}_3$ (4)	Dry toluene	Xe	5 h	94%	100%
9	NHC(Cu)-PCMP(Cu) (10mg)	$t\text{BuNH}_2\text{BH}_3$ (4)	toluene	Xe	5 h	94%	100%
10	NHC(Cu)-PCMP (10 mg)	$t\text{BuNH}_2\text{BH}_3$ (4)	toluene	Xe	5 h	71%	100%
11	Im-PCMP (10 mg)	$t\text{BuNH}_2\text{BH}_3$ (4)	toluene	Xe	5 h	28%	100%
12 ^c	NHC(Cu)-PCMP(Cu) (10mg)	$t\text{BuNH}_2\text{BH}_3$ (4)	toluene	R.t.	5 h	29%	100%
13 ^c	NHC(Cu)-PCMP(Cu) (10mg)	$t\text{BuNH}_2\text{BH}_3$ (4)	toluene	80°C	5 h	99%	100%
14 ^c	NHC(Cu)-PCMP(Cu) (10mg)	$t\text{BuNH}_2\text{BH}_3$ (4)	toluene	75°C	5 h	85%	100%
15 ^c	NHC(Cu)-PCMP(Cu) (10mg)	$t\text{BuNH}_2\text{BH}_3$ (4)	toluene	50°C	5 h	29%	100%
16 ^d	NHC(Cu)-PCMP(Cu) (10mg)	$t\text{BuNH}_2\text{BH}_3$ (4)	toluene	R.t.	5 h	28%	100%
17	NHC(Cu) (10 mg)	$t\text{BuNH}_2\text{BH}_3$ (4)	toluene	Xe	5 h	-	-
18	Por(Cu) (10mg)	$t\text{BuNH}_2\text{BH}_3$ (4)	toluene	Xe	5 h	-	-
19	---	$t\text{BuNH}_2\text{BH}_3$ (4)	toluene	Xe	5 h	-	-
20	$\text{Pd}(\text{PPh}_3)_4$ (2 mg)	$t\text{BuNH}_2\text{BH}_3$ (4)	toluene	Xe	5 h	-	-

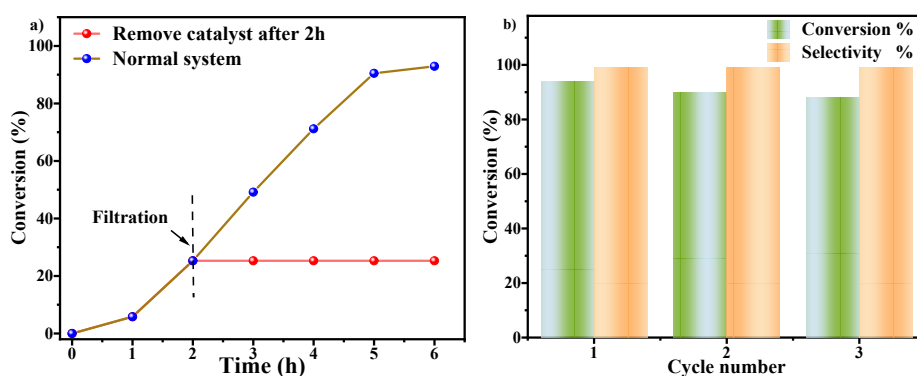
^a Reaction condition: **1a** (0.2 mmol), Hydride, solvent (2 mL), 300 W Xe lamp ($\lambda > 420\text{nm}$), N_2 ball;

^b Conversion and selectivity determined by GC-MS, the selectivity was reflected in parentheses;

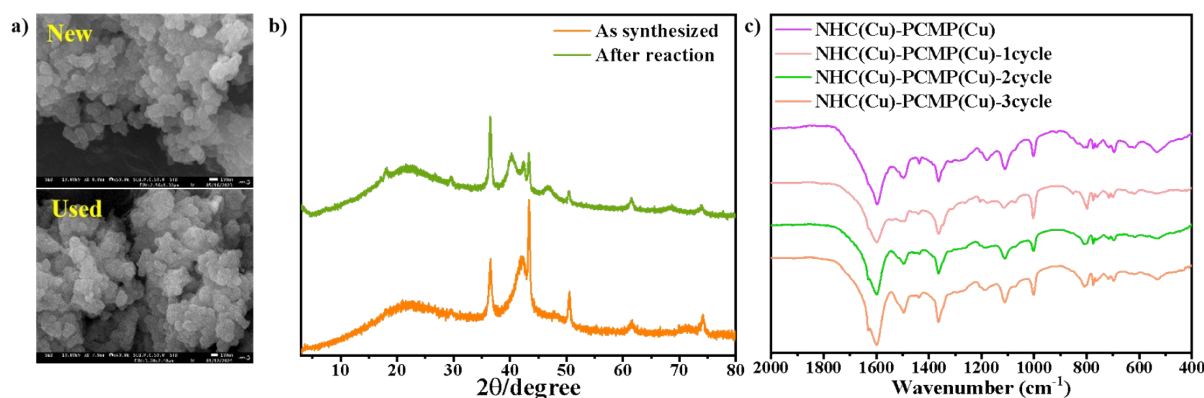
^c Dark conditions;

^d 300 W Xe lamp ($\lambda > 420\text{nm}$), maintaining room temperature with condensate water.

3. Hot filtration experiment and recycling experiments. (Figure S18)



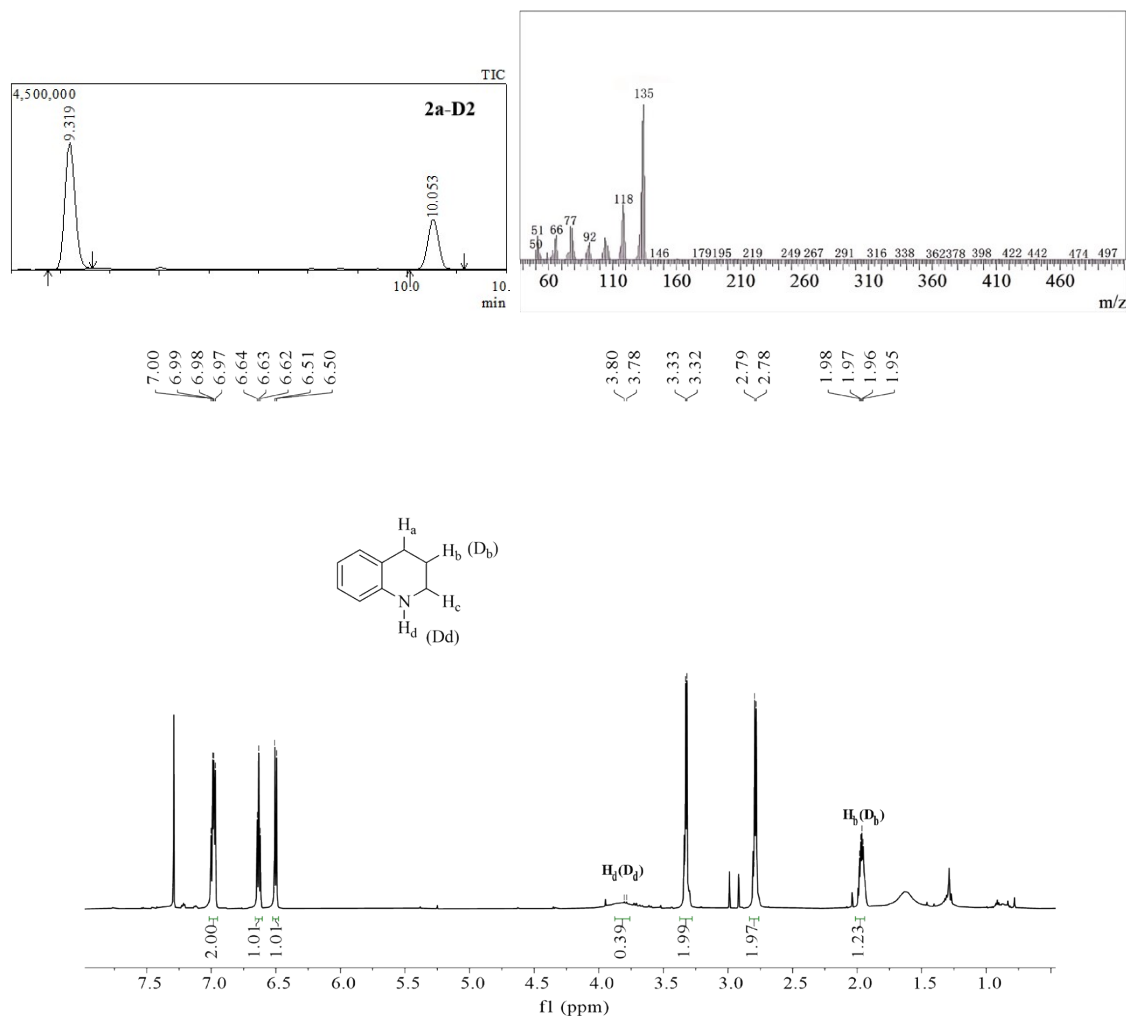
4. The SEM images, PXRD and IR spectra for NHC(Cu)-PCMP(Cu) of the as-synthesized sample and after the 3th runs of the transfer hydrogenation reactions. (Figure S19)



5. Comparison of the photo-thermal reduction with previous reports. (Table S2)

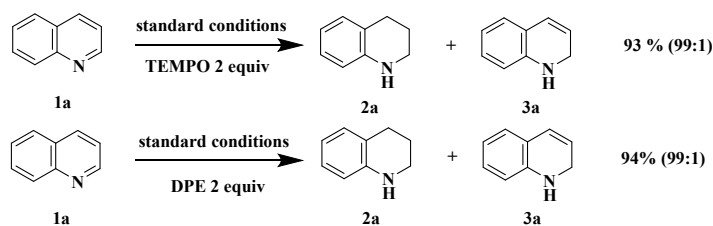
Entry	Catalyst	Condition	Conversion	Ref.
1	$\text{Co}_3\text{Cu}_1\text{Ox}$	H_2 , 4 MPa	>99%	8
2	$2\text{Ir}_n/\text{SC}$	100 °C, 2 MPa H_2	>99%	9
3	$\text{Fe}_4\text{Ni}_6\text{Cu}_5/\text{MCM-41}$	H_2 , 4 MPa, 50-80°C	>90%	10
4	ZCT-3 ($\text{Cu}_3@\text{Zn-TiO}_2$)	H_2 balloon, 125W halogen lamp	87%	11
5	$\text{Pd}@\text{ompg-C}_3\text{N}_4$	H_2 1 bar, 100 °C	>99%	12
6	Ni-bipy-COF	NH_3BH_3 (5.0 eq.), 90°C	62-98%	13
7	<i>NHC(Cu)-PCMP(Cu)</i>	<i>t-NH₂BH₃</i> (4 eq.), 300 W Xe lamp	65-100%	This work

6. The GC-MS and ¹H NMR spectra for 2a-D2 in deuterium-labeled experiments. (Figure S20)

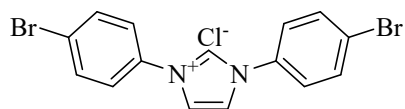


7. Free radical experiments

In a typical reaction, **NHC(Cu)-PCMP(Cu)** (10 mg) was used as catalyst, **1a** (0.2 mmol) and *t*-BuNH₂BH₃ (0.8 mmol) and TEMPO / DPE (0.4 mmol) were dispersed in toluene (2.0 mL) in 5 mL branched Schlenk tube, which were irradiated with a 300W Xe lamp for 5 hours under N₂ atmosphere. After the reaction was finished, the yield was determined by GC-MS.

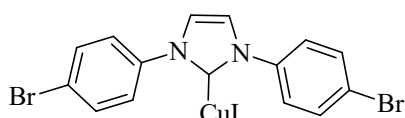


Section 5. NMR data of monomer and products



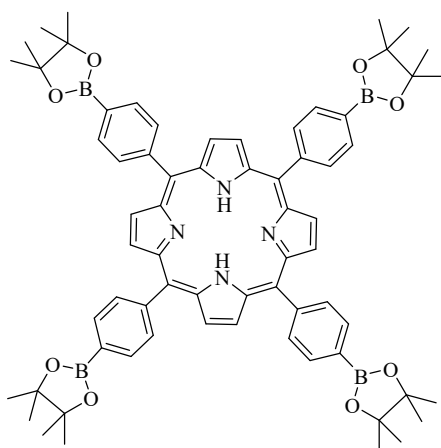
1,3-Bis(4-bromophenyl)-1H-imidazol-3-chloride (Im)

^1H NMR (600 MHz, DMSO) δ 10.43 (s, 1H), 8.60 (s, 2H), 7.97 (d, $J = 9.0$ Hz, 4H), 7.90 (d, $J = 9.0$ Hz, 4H). ^{13}C NMR (151 MHz, CDCl_3) δ 135.8, 134.5, 133.6, 124.9, 123.6, 122.3.



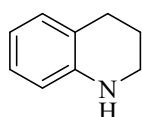
(1,3-bis(4-bromophenyl)-2,3-dihydro-2-yl)copper(I) iodide (NHC(Cu))

^1H NMR (600 MHz, DMSO) δ 8.05 (s, 2H), 7.86 (s, 4H), 7.73 (s, 4H). ^{13}C NMR (151 MHz, DMSO) δ 139.2, 133.6, 132.8, 132.4, 125.8, 124.6, 123.5, 122.7, 121.7. HRMS (ESI): calculated for $\text{C}_{15}\text{H}_{11}\text{Br}_2\text{CuIN}_2$ ($\text{M} + \text{H}^+$) requires 566.7630, found: 566.7639. Anal. Calcd for $\text{C}_{15}\text{H}_{10}\text{Br}_2\text{CuIN}_2$ (Mr-565.7551): C, 31.69%; H, 1.77%; N, 4.93%; Cu, 11.18%; I, 22.32%; Br, 28.11%. Found: C, 31.95%; H, 1.63%; N, 4.93%; Cu, 11.68%; I, 22.02%; Br, 27.79%.



5,10,15,20-Tetrakis(4-borate pinacol phenyl)porphyrin (Por)

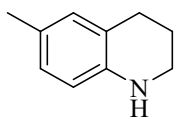
^1H NMR (600 MHz, CDCl_3) δ 8.82 (s, 8H), 8.22 (d, $J = 7.8$ Hz, 8H), 8.18 (d, $J = 7.8$ Hz, 8H), 1.50 (s, 48H).



1,2,3,4-tetrahydroquinoline (2a)¹⁴

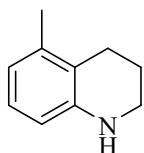
^1H NMR (600 MHz, CDCl_3) δ 7.04 – 6.95 (m, 2H), 6.65 (d, $J = 7.3$ Hz, 1H), 6.51 (d, $J = 7.9$ Hz, 1H), 3.85 (s, 1H), 3.37

- 3.31 (m, 2H), 2.80 (t, $J = 6.4$ Hz, 2H), 2.03 – 1.95 (m, 2H). ^{13}C NMR (151 MHz, CDCl_3) δ 144.7, 129.5, 126.7, 121.4, 116.9, 114.1, 41.9, 26.9, 22.1. HRMS (ESI) m/z calculated for $\text{C}_9\text{H}_{12}\text{N}$ ($[\text{M} + \text{H}]^+$): 134.0964, found 134.0965.



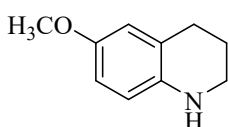
6-methyl-1,2,3,4-tetrahydroquinoline (2b)¹⁴

^1H NMR (600 MHz, CDCl_3) δ 6.89 (d, $J = 6.0$ Hz, 2H), 6.52 – 6.50 (t, $J = 8.4$ Hz, $J = 5.4$ Hz, 1H), 3.78 (s, 1H), 3.38 – 3.36 (t, $J = 10.8$ Hz, $J = 5.4$ Hz, 2H), 2.84 – 2.83 (t, $J = 13.2$ Hz, $J = 6.6$ Hz, 2H), 2.31 (s, 3H), 2.04 – 2.02 (t, $J = 10.4$ Hz, $J = 5.4$ Hz, 2H). ^{13}C NMR (151 MHz, CDCl_3) δ 142.4, 130.0, 127.2, 126.2, 121.6, 114.4, 42.1, 26.9, 22.4, 20.4. HRMS (ESI) m/z calculated for $\text{C}_{10}\text{H}_{14}\text{N}$ ($[\text{M} + \text{H}]^+$): 148.1121, found 148.1121.



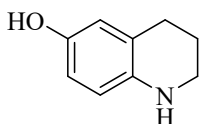
5-methyl-1,2,3,4-tetrahydroquinoline (2c)¹⁴

^1H NMR (600 MHz, CDCl_3) δ 7.26 (s, 1H), 6.91 – 6.88 (m, 1H), 6.53 (d, $J = 7.2$ Hz, 1H), 6.38 (d, $J = 7.5$ Hz, 1H), 3.28 – 3.25 (t, $J = 11.4$ Hz, $J = 5.4$ Hz, 2H), 2.66 – 2.64 (t, $J = 13.2$ Hz, $J = 6.6$ Hz, 2H), 2.19 (s, 3H), 2.01 – 1.99 (m, 2H). ^{13}C NMR (151 MHz, CDCl_3) δ 144.9, 137.2, 126.1, 120.2, 118.9, 112.4, 41.5, 24.0, 22.5, 19.3. HRMS (ESI) m/z calculated for $\text{C}_{10}\text{H}_{14}\text{N}$ ($[\text{M} + \text{H}]^+$): 148.1121, found 148.1123.



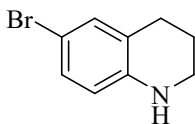
6-methoxy-1,2,3,4-tetrahydroquinoline (2d)¹⁴

^1H NMR (600 MHz, CDCl_3) δ 6.60 – 6.56 (m, 2H), 6.46 (d, $J = 8.4$ Hz, 1H), 3.73 (s, 3H), 3.27 – 3.25 (t, $J = 10.8$ Hz, $J = 5.4$ Hz, 2H), 2.76 (t, $J = 12.0$ Hz, $J = 6.0$ Hz, 2H), 1.95 – 1.91 (m, 2H). ^{13}C NMR (151 MHz, CDCl_3) δ 151.9, 138.7, 122.9, 115.6, 114.9, 112.9, 55.8, 42.3, 27.1, 22.4. HRMS (ESI) m/z calculated for $\text{C}_{10}\text{H}_{14}\text{NO}$ ($[\text{M} + \text{H}]^+$): 164.1070, found 164.1070.



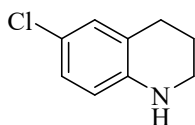
6-methoxy-1,2,3,4-tetrahydroquinoline (2e) ¹⁴

¹H NMR (600 MHz, CDCl₃) δ 6.50 (d, *J* = 10.2 Hz, 2H), 6.40 (d, *J* = 8.4 Hz, 1H), 3.26 – 3.24 (t, *J* = 10.2 Hz, *J* = 5.4 Hz, 2H), 2.73 – 2.72 (t, *J* = 12.0 Hz, *J* = 6.0 Hz, 2H), 1.93 – 1.91 (t, *J* = 11.4 Hz, *J* = 6.0 Hz, 2H). ¹³C NMR (151 MHz, DMSO) δ 147.8, 138.1, 121.2, 115.5, 114.8, 113.5, 41.3, 26.7, 22.1. HRMS (ESI) *m/z* calculated for C₉H₁₂NO ([M + H]⁺): 150.0913, found 150.0914.



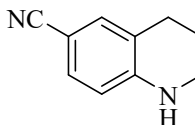
6-bromo-1,2,3,4-tetrahydroquinoline (2f) ¹⁴

¹H NMR (600 MHz, CDCl₃) δ 7.05 – 7.01 (m, 2H), 6.34 (d, *J* = 8.4 Hz, 1H), 3.83 (s, 1H), 3.29 – 3.27 (t, *J* = 10.8 Hz, *J* = 5.4 Hz, 2H), 2.74 – 2.71 (t, *J* = 12.0 Hz, *J* = 6.0 Hz, 2H), 1.92 – 1.90 (t, *J* = 12.0 Hz, *J* = 6.0 Hz, 2H). ¹³C NMR (151 MHz, CDCl₃) δ 143.7, 131.8, 129.3, 123.4, 115.5, 108.2, 41.8, 26.8, 21.7. HRMS (ESI) *m/z* calculated for C₉H₁₁NBr ([M + H]⁺): 212.0069, found 212.0070.



6-chloro-1,2,3,4-tetrahydroquinoline (2g) ¹⁴

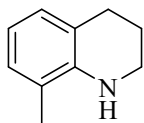
¹H NMR (600 MHz, CDCl₃) δ 6.90 (d, *J* = 10.8 Hz, 2H), 6.38 (d, *J* = 8.4 Hz, 1H), 3.82 (s, 1H), 3.29 – 3.27 (t, *J* = 10.8 Hz, *J* = 5.4 Hz, 2H), 2.74 – 2.71 (t, *J* = 12.0 Hz, *J* = 6.0 Hz, 2H), 1.92 – 1.90 (t, *J* = 12.0 Hz, *J* = 6.0 Hz, 2H). ¹³C NMR (151 MHz, CDCl₃) δ 143.3, 129.0, 126.5, 122.8, 121.1, 115.0, 41.8, 26.8, 21.7. HRMS (ESI) *m/z* calculated for C₉H₁₁NCl ([M + H]⁺): 168.0575, found 168.0578.



6-carbonitrile-1,2,3,4-tetrahydroquinoline (2h) ¹⁴

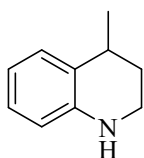
¹H NMR (600 MHz, CDCl₃) δ 7.28 – 7.19 (m, 2H), 6.41 (d, *J* = 8.4 Hz, 1H), 4.46 (s, 1H), 3.38 (t, *J* = 9.6 Hz, *J* = 4.8 Hz, 2H), 2.74 (t, *J* = 12.6 Hz, *J* = 6.6 Hz, 2H), 1.95 – 1.91 (m, 2H). ¹³C NMR (151 MHz, CDCl₃) δ 148.3, 133.1 (d), 131.2 (d), 120.9, 113.3 (m), 97.6, 41.6 (t), 26.7 (t), 21.0 (t). HRMS (ESI) *m/z* calculated for C₁₀H₁₁N₂ ([M + H]⁺):

159.0917, found 159.0920.



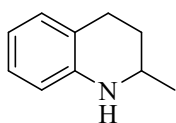
8-methyl-1,2,3,4-tetrahydroquinoline (2i)¹⁴

¹H NMR (600 MHz, CDCl₃) δ 6.96 (d, *J* = 7.8 Hz, 1H), 6.94 (d, *J* = 7.8 Hz, 1H), 6.66 – 6.64 (m, 1H), 3.87 (s, 1H), 3.46 (t, *J* = 9.6 Hz, *J* = 4.8 Hz, 2H), 2.88 (t, *J* = 12.0 Hz, *J* = 6.0 Hz, 2H), 2.17 (s, 3H), 2.05 – 2.01 (m, 2H). ¹³C NMR (151 MHz, CDCl₃) δ 142.8, 127.9 (d), 127.4 (d), 121.2 (d), 120.9 (d), 116.3 (d), 42.4 (t), 27.4, 22.2 (t), 17.1 (m). HRMS (ESI) *m/z* calculated for C₁₀H₁₄N ([M + H]⁺): 148.1121, found 148.1123.



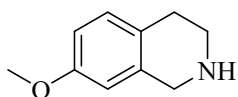
4-methyl-1,2,3,4-tetrahydroquinoline (2j)¹⁴

¹H NMR (600 MHz, CDCl₃) δ 7.12 (t, *J* = 17.4 Hz, *J* = 9.0 Hz, 1H), 7.02 (t, *J* = 16.8 Hz, *J* = 9.0 Hz, 1H), 6.72 – 6.68 (m, 1H), 6.55 – 6.52 (m, 1H), 3.49 (s, 1H), 3.39 – 3.31 (m, 2H), 2.98 (t, *J* = 10.8 Hz, *J* = 6.0 Hz, 1H), 2.05 (t, *J* = 7.2 Hz, *J* = 3.6 Hz, 1H), 1.74 (t, *J* = 10.2 Hz, *J* = 3.6 Hz, 1H), 1.36 (dd, *J* = 10.8 Hz, *J* = 7.2 Hz, 3H). ¹³C NMR (151 MHz, CDCl₃) δ 144.3, 128.5 (t), 126.7 (t), 117.1, 116.9, 114.2 (t), 39.1 (t), 30.3 (t), 29.9, 22.8 (d). HRMS (ESI) *m/z* calculated for C₁₀H₁₄N ([M + H]⁺): 148.1121, found 148.1122.



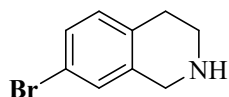
2-methyl-1,2,3,4-tetrahydroquinoline (2k)¹⁴

¹H NMR (600 MHz, CDCl₃) δ 7.02 – 6.99 (m, 2H), 6.65 (t, *J* = 13.2 Hz, *J* = 6.0 Hz, 1H), 6.51 (d, *J* = 8.4 Hz, 1H), 3.74 (s, 1H), 3.43 (m, 1H), 2.86 (m, 1H), 2.78 (m, 1H), 1.96 (m, 1H), 1.63 (m, 1H), 1.25 (d, *J* = 6.6, *J* = 4.2, 3H). ¹³C NMR (151 MHz, CDCl₃) δ 144.8, 129.3 (d), 126.7 (d), 121.1 (d), 117.0 (d), 113.7 (d), 47.3 (d), 30.1 (d), 26.7, 22.7 (d). HRMS (ESI) *m/z* calculated for C₁₀H₁₄N ([M + H]⁺): 148.1121, found 148.1121.



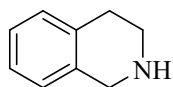
7-methoxy-1,2,3,4-tetrahydroisoquinoline (2l)

^1H NMR (600 MHz, CDCl_3) δ 6.96 (d, $J = 8.4$ Hz, 1H), 6.68 (d, $J = 8.4$ Hz, 1H), 6.51 (s, 1H), 3.92 (s, 2H), 3.72 (s, 3H), 3.05 (t, $J = 12.0$ Hz, $J = 6.0$ Hz, 2H), 2.67 (t, $J = 12.0$ Hz, $J = 5.4$ Hz, 2H), 2.38 (s, 1H). ^{13}C NMR (151 MHz, CDCl_3) δ 157.6, 136.8, 130.1(d), 126.7, 112.4 (d), 110.8 (t), 55.2 (m), 48.4 (t), 44.0, 28.3 (m). HRMS (ESI) m/z calculated for $\text{C}_{10}\text{H}_{14}\text{NO}$ ($[\text{M} + \text{H}]^+$): 164.1070, found 164.1073.



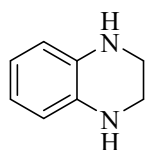
7-bromo-1,2,3,4-tetrahydroisoquinoline (2m)

^1H NMR (600 MHz, CDCl_3) δ 7.25 – 7.23 (dd, $J = 7.8, 1.8$ Hz, 1H), 7.16 (s, 1H), 6.96 (d, $J = 7.8$ Hz, 1H), 3.97 (s, 2H), 3.11 (t, $J = 11.4$ Hz, $J = 6.0$ Hz, 2H), 2.73 (t, $J = 11.4$ Hz, $J = 6.0$ Hz, 2H). ^{13}C NMR (151 MHz, CDCl_3) δ 138.1, 133.8, 131.0, 129.0, 119.2, 48.0, 43.6, 28.7. HRMS (ESI) m/z calculated for $\text{C}_9\text{H}_{10}\text{NBr}$ ($[\text{M} + \text{H}]^+$): 212.0069, found 212.0070.



1,2,3,4-tetrahydroisoquinoline (2n)

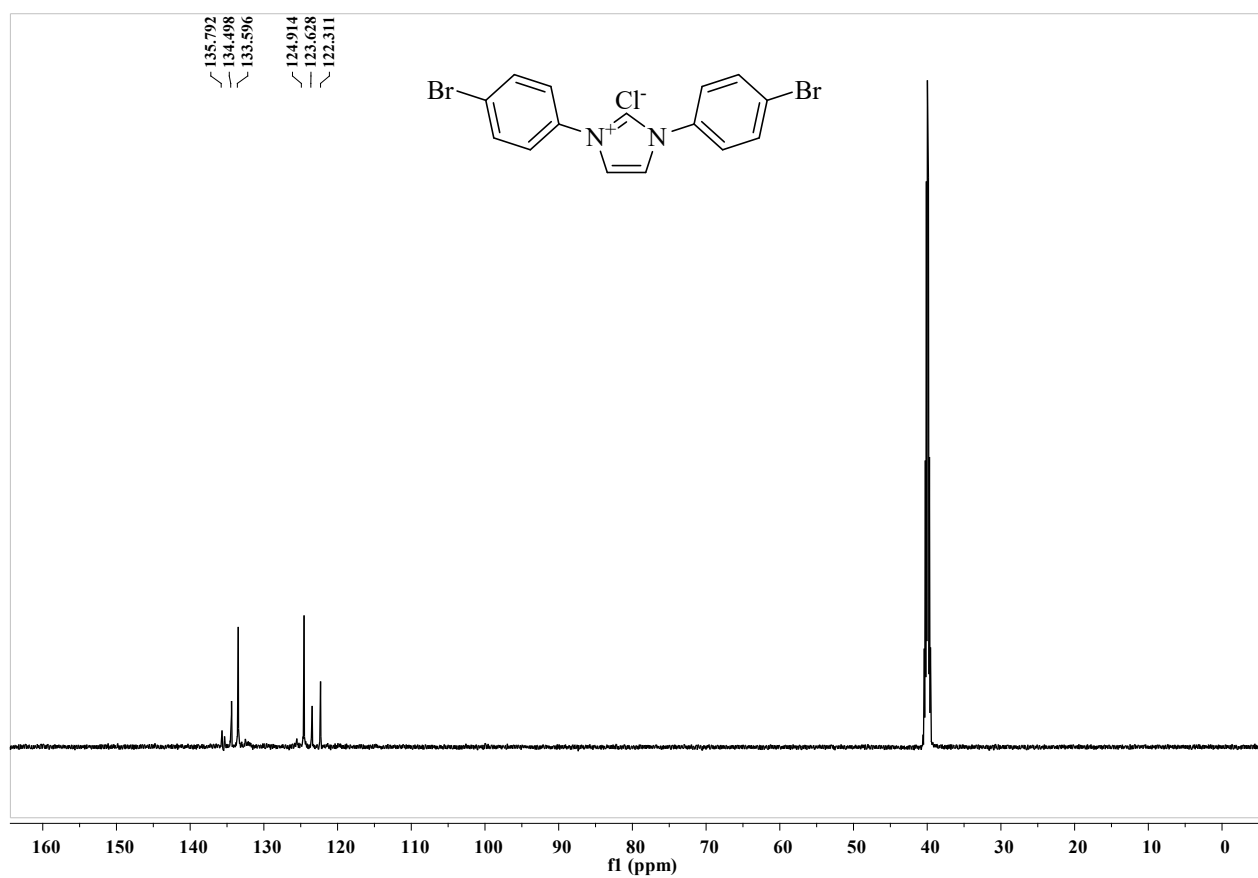
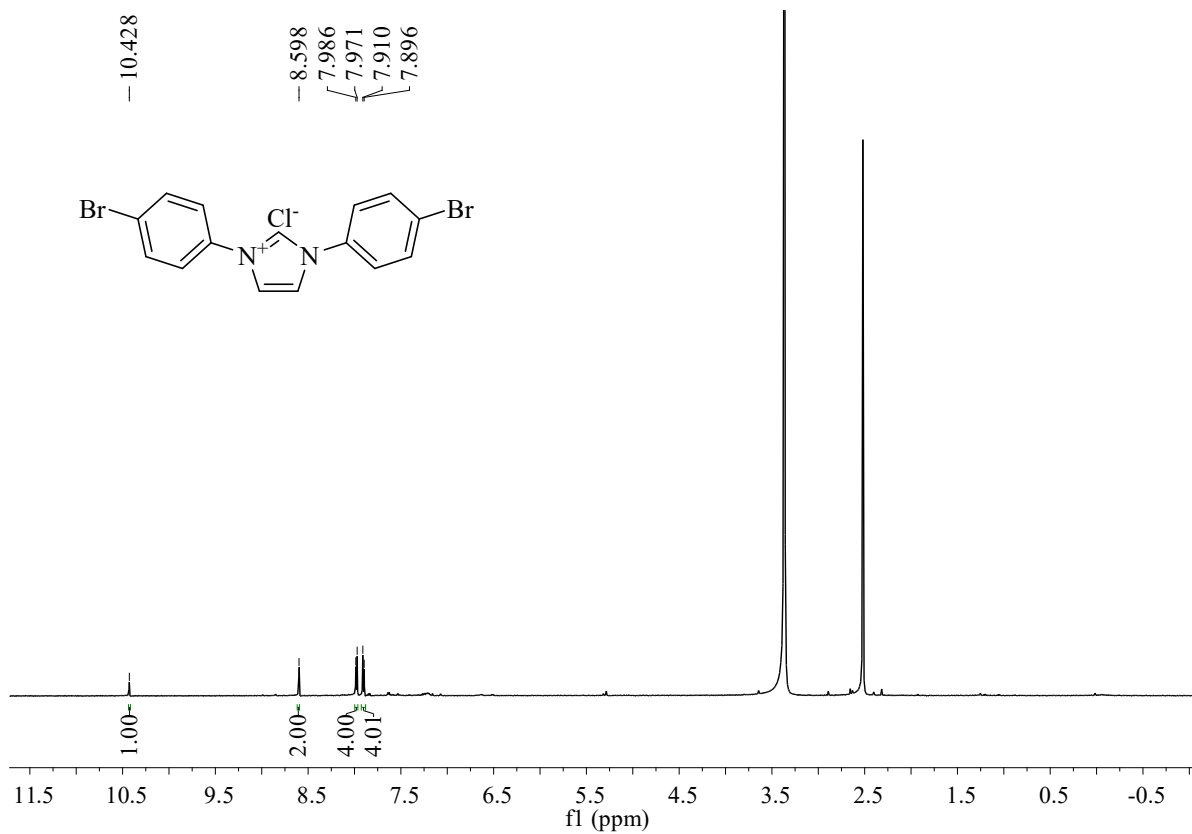
^1H NMR (600 MHz, CDCl_3) δ 7.25 – 7.23 (dd, $J = 7.8, 1.8$ Hz, 1H), 7.16 (s, 1H), 6.96 (d, $J = 7.8$ Hz, 1H), 3.97 (s, 2H), 3.11 (t, $J = 11.4$ Hz, $J = 6.0$ Hz, 2H), 2.73 (t, $J = 11.4$ Hz, $J = 6.0$ Hz, 2H). ^{13}C NMR (151 MHz, CDCl_3) δ 135.9, 134.8, 129.3, 126.2, 126.0, 125.7, 48.3 (t), 43.9, 29.2. HRMS (ESI) m/z calculated for $\text{C}_9\text{H}_{12}\text{N}$ ($[\text{M} + \text{H}]^+$): 134.0964, found 134.0960.

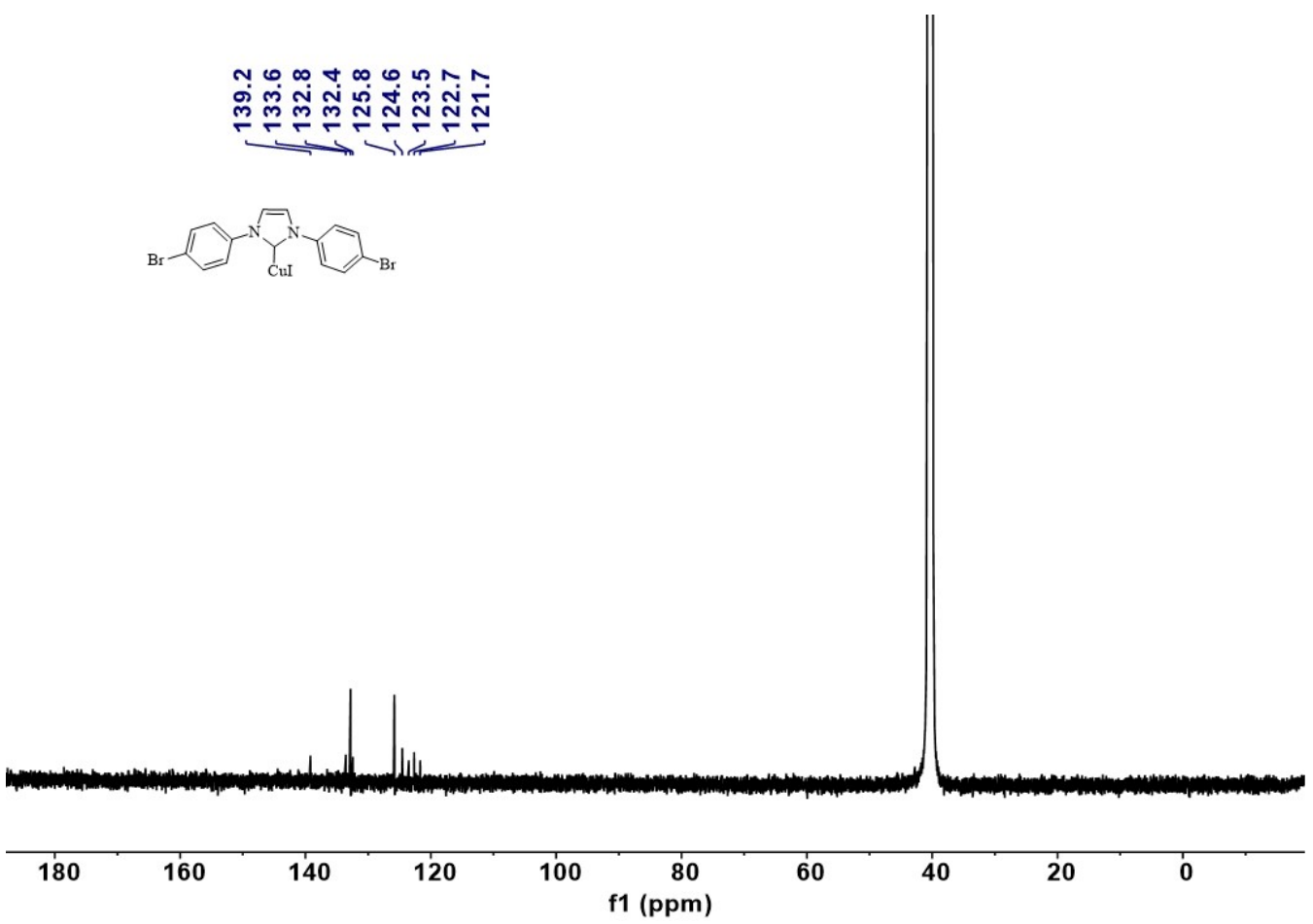
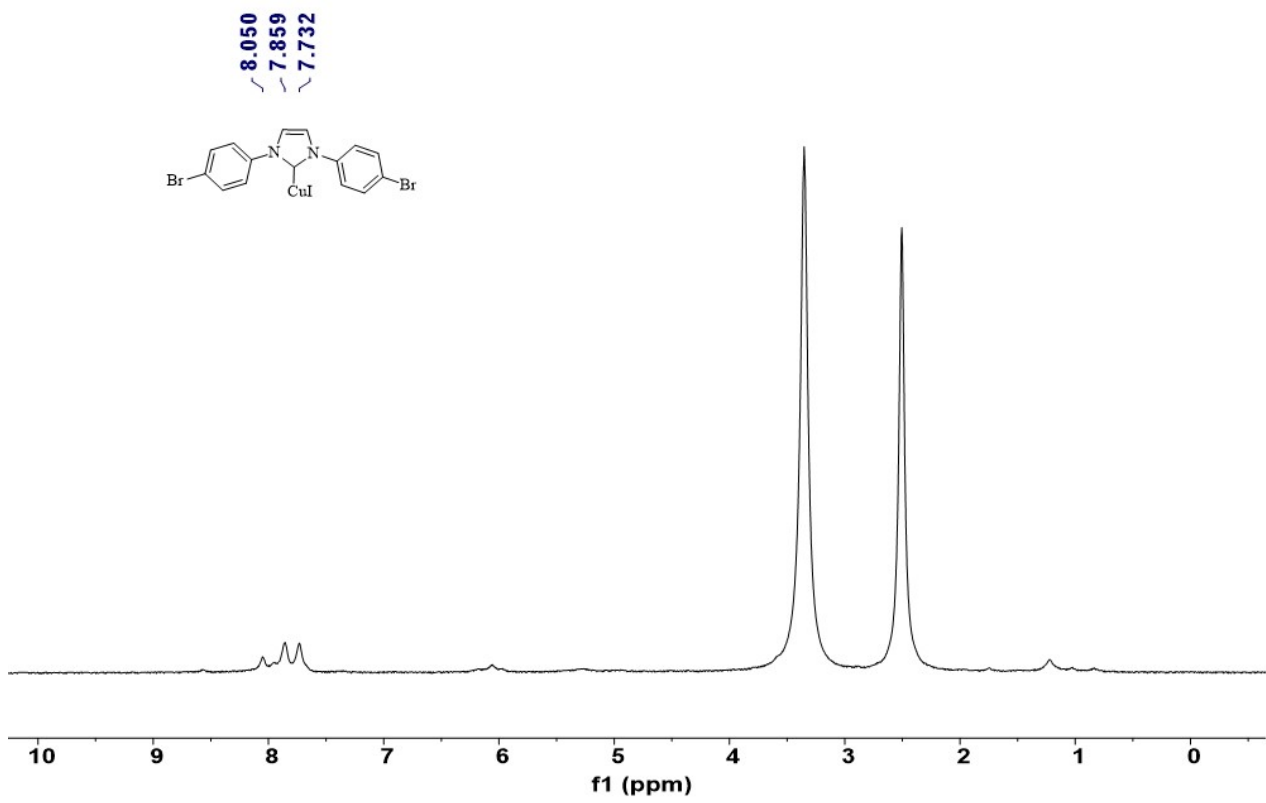


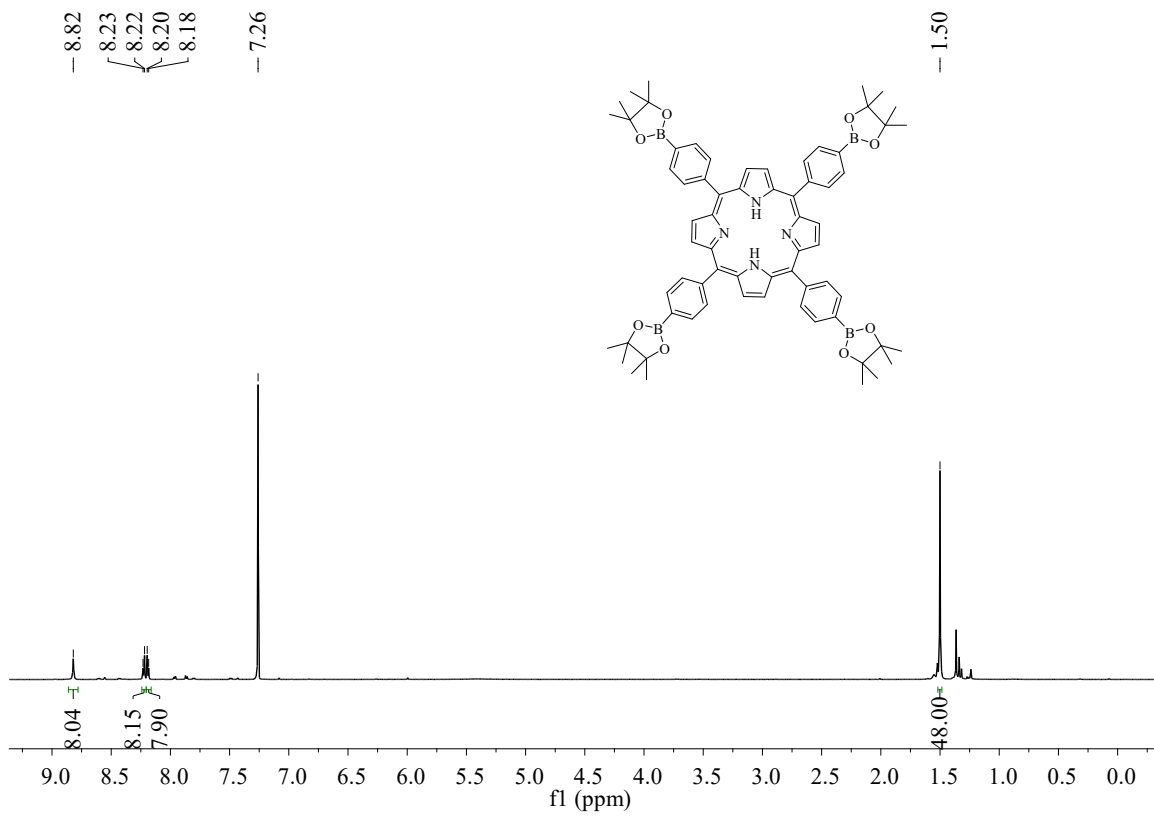
1,2,3,4-tetrahydroquinoxaline (2o)

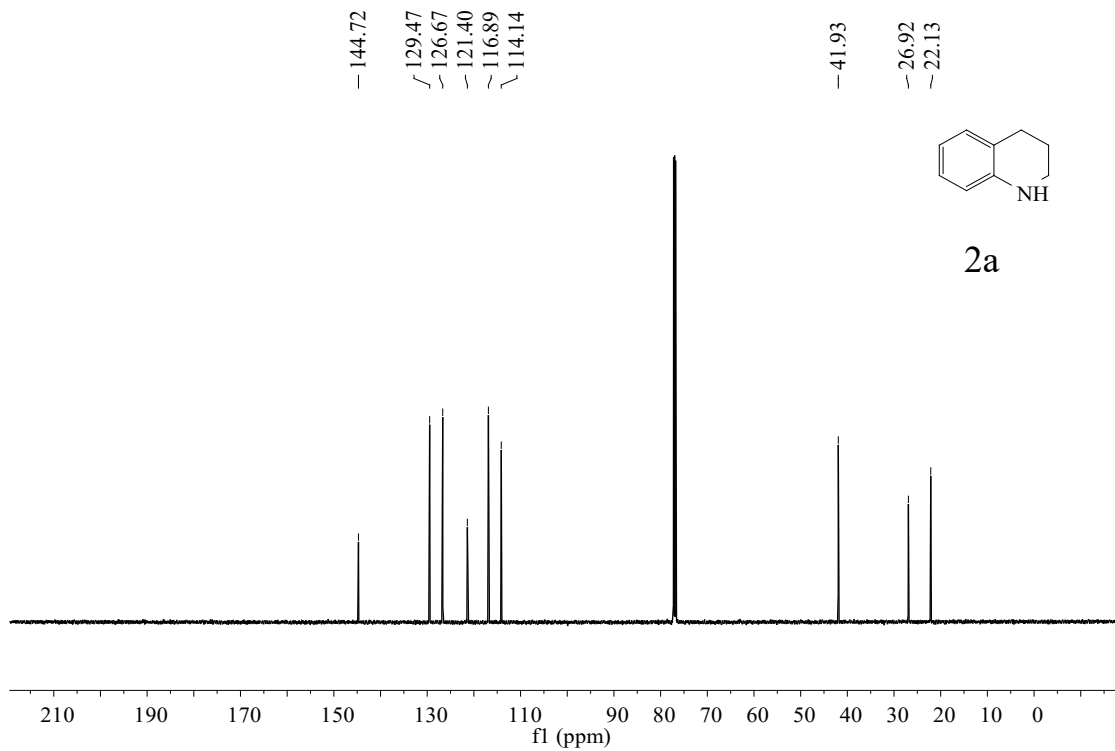
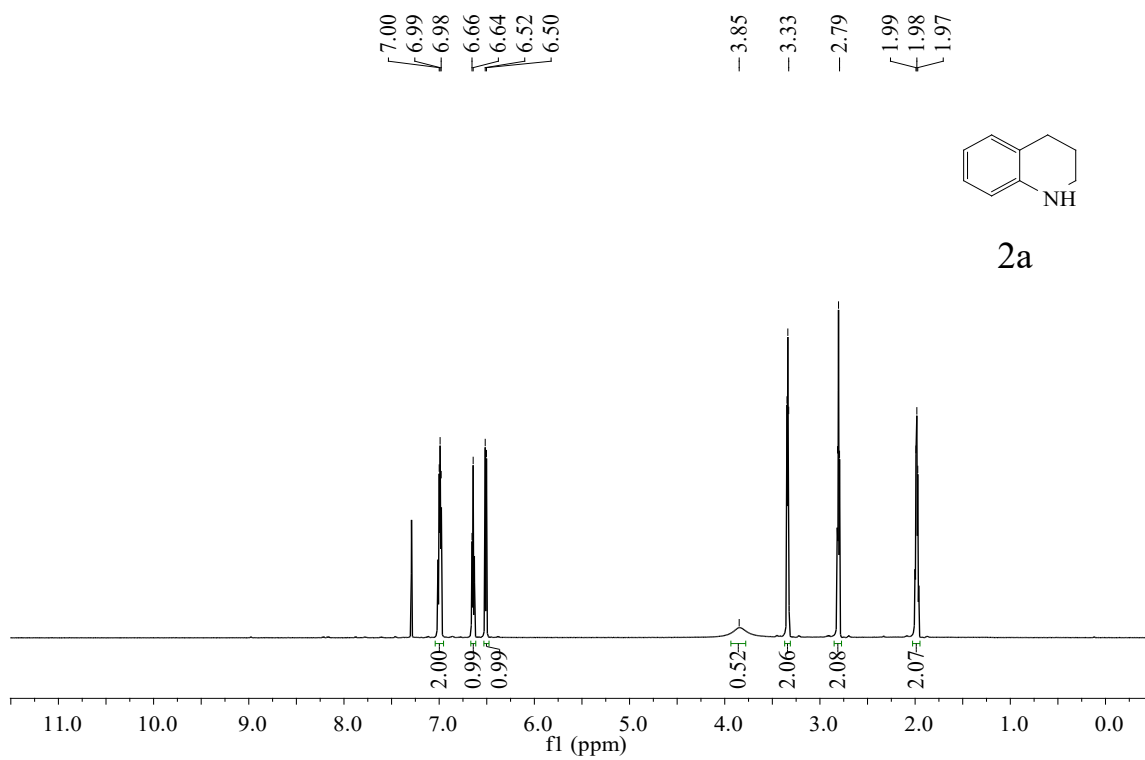
^1H NMR (600 MHz, CDCl_3) δ 6.61 – 6.58 (m, 2H), 6.52 – 6.49 (m, 2H), 3.64 (s, 2H), 3.42 (s, 4H). ^{13}C NMR (151 MHz, CDCl_3) δ 133.7, 118.8, 118.7, 115.1, 114.7, 114.4, 41.7, 41.4. HRMS (ESI) m/z calculated for $\text{C}_9\text{H}_{12}\text{N}$ ($[\text{M} + \text{H}]^+$): 135.0917, found 135.0920.

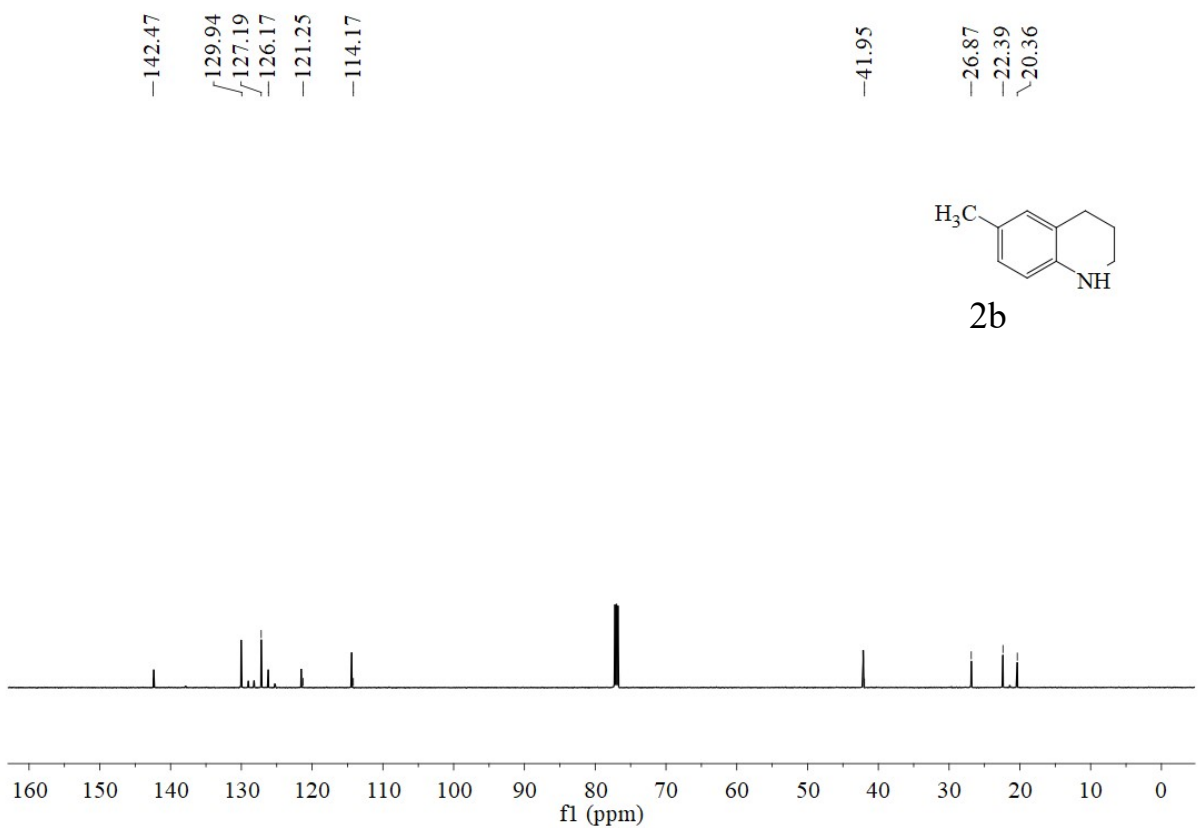
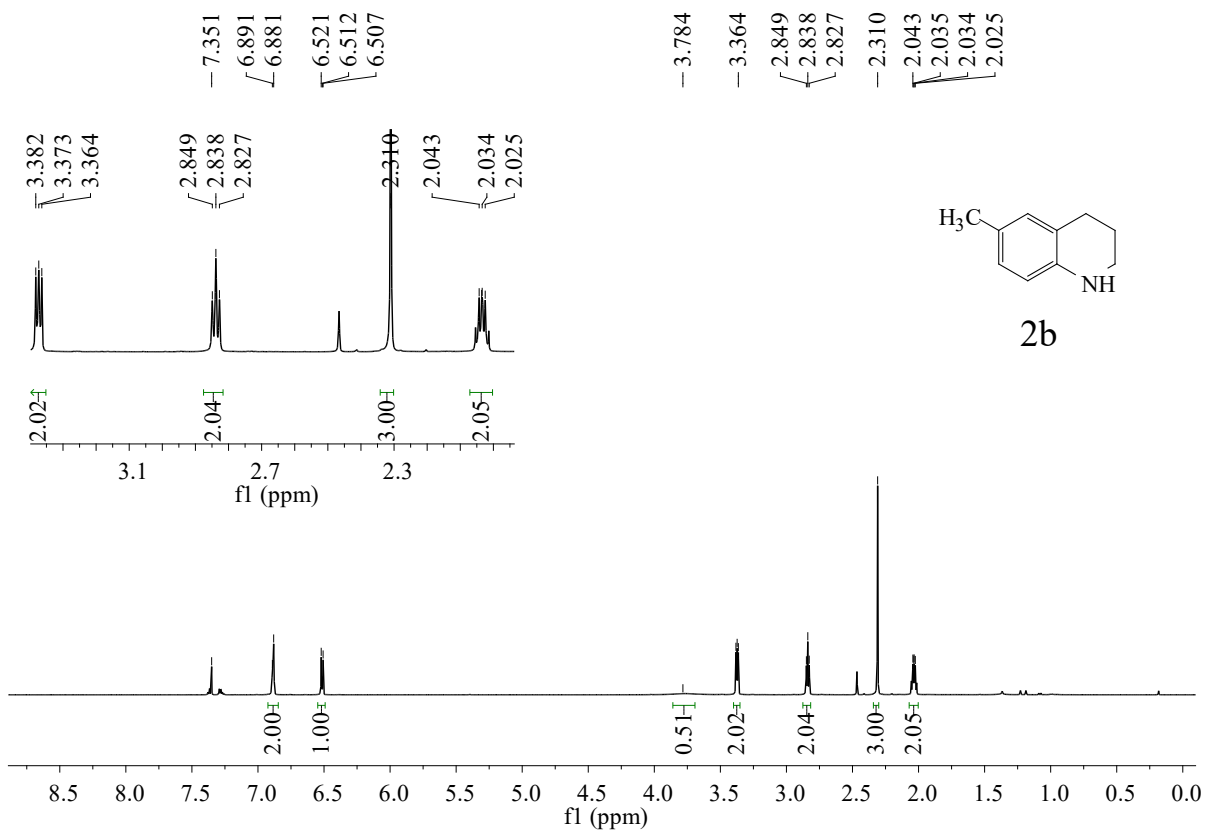
Section 6. NMR spectra of products

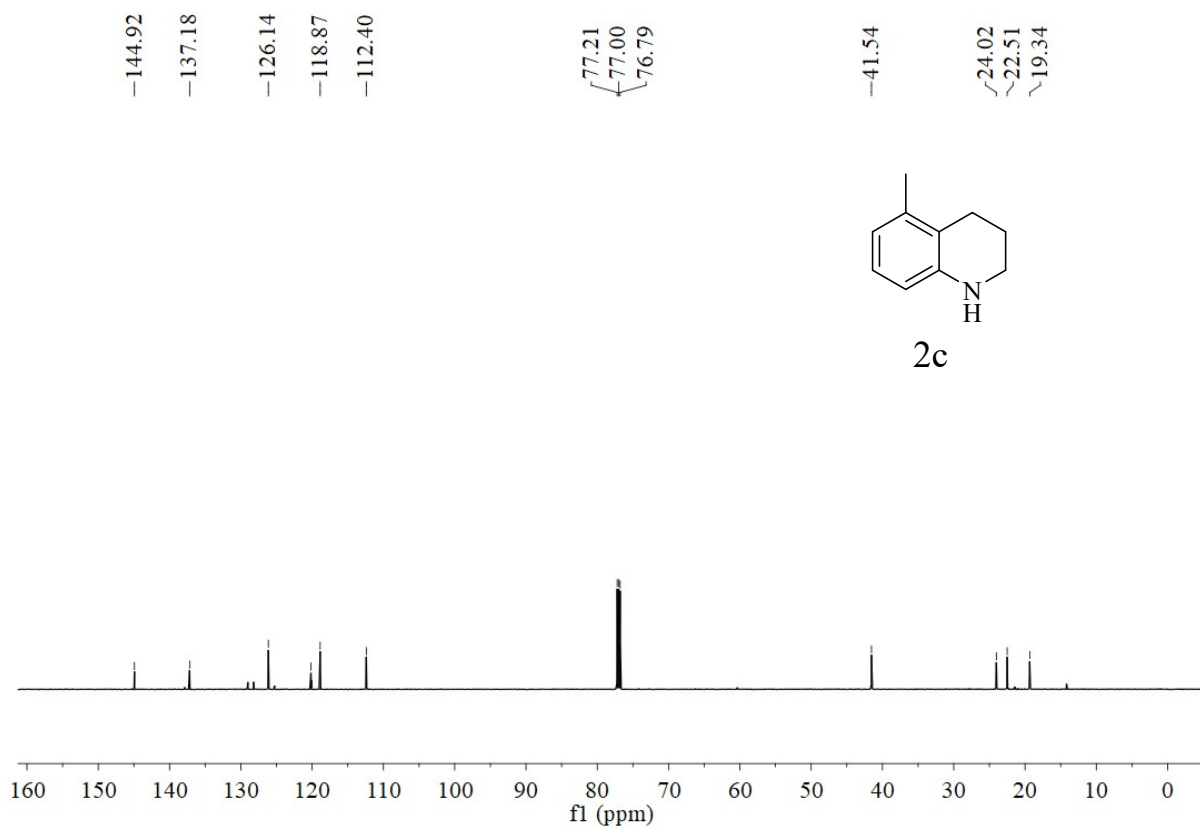
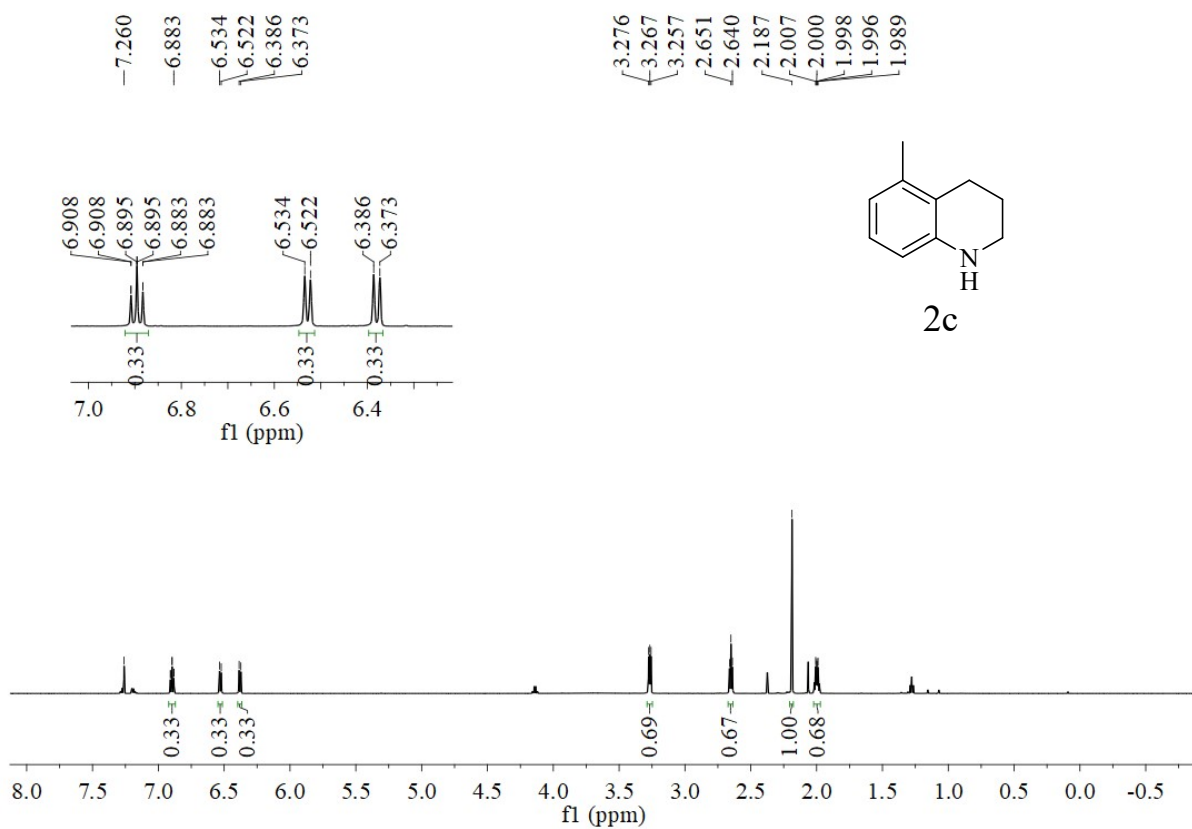


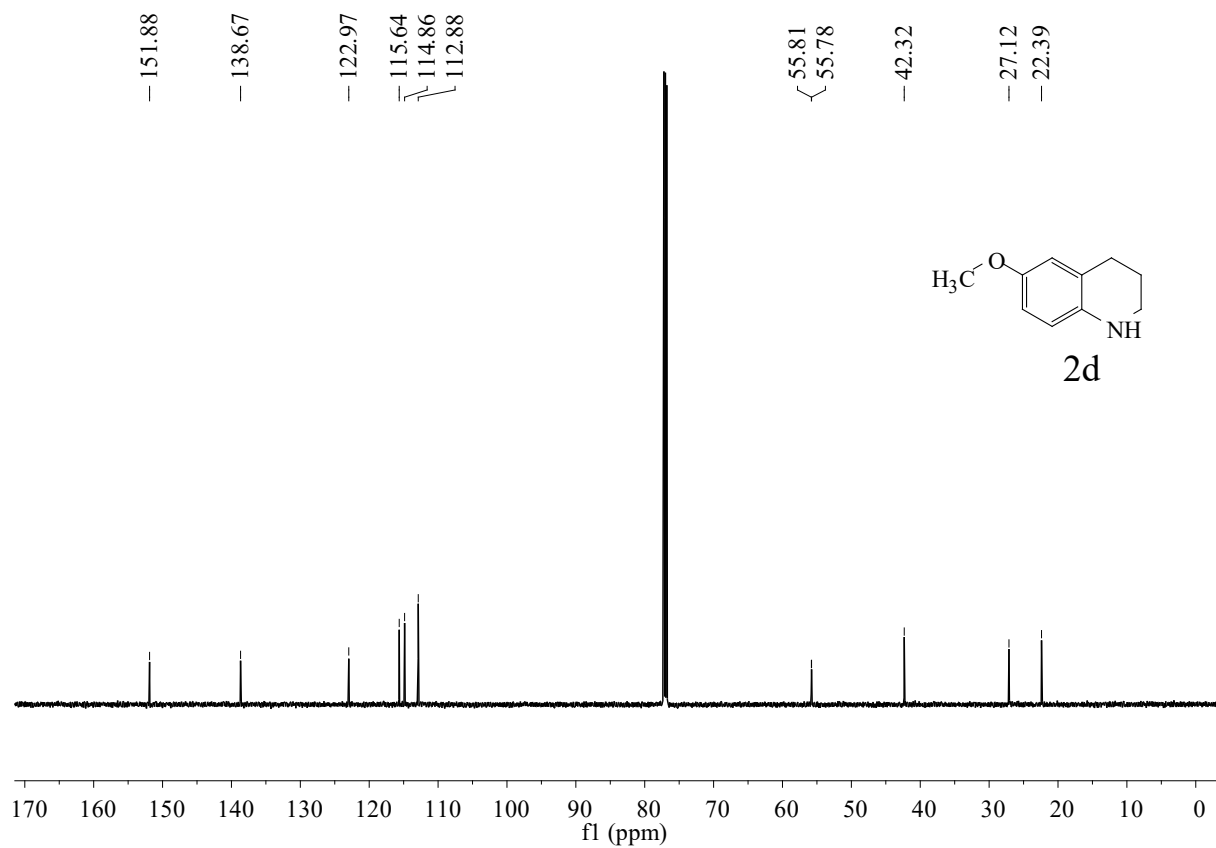
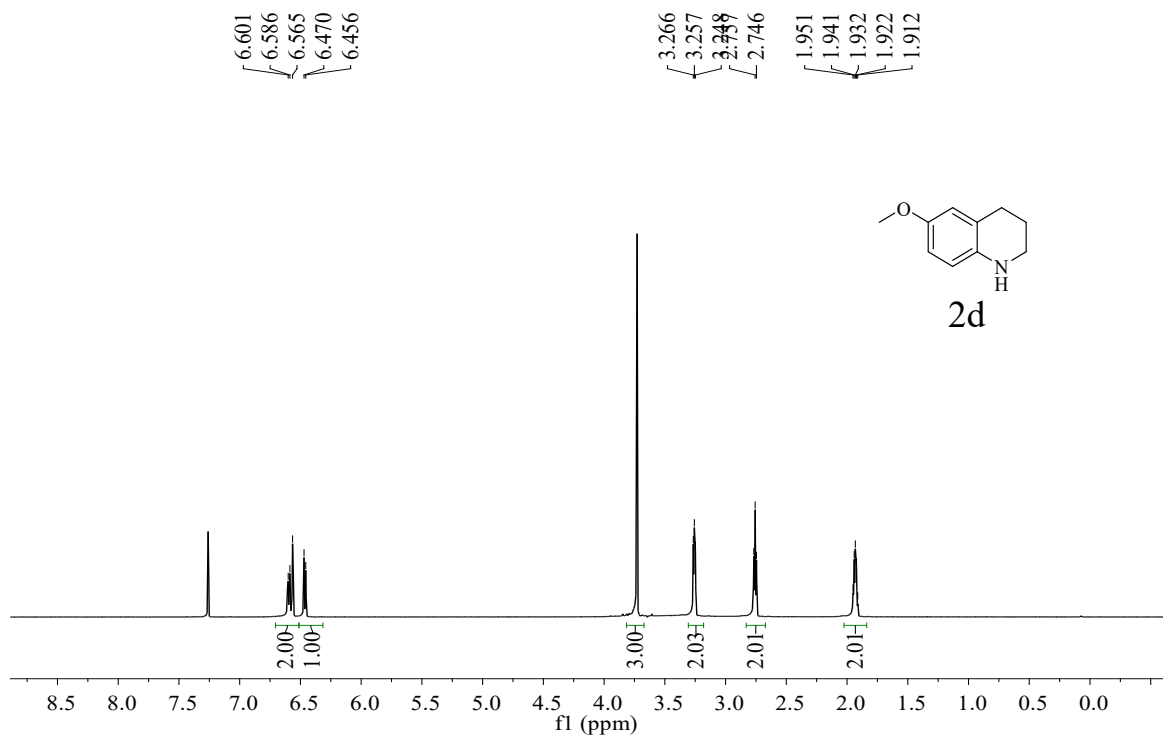


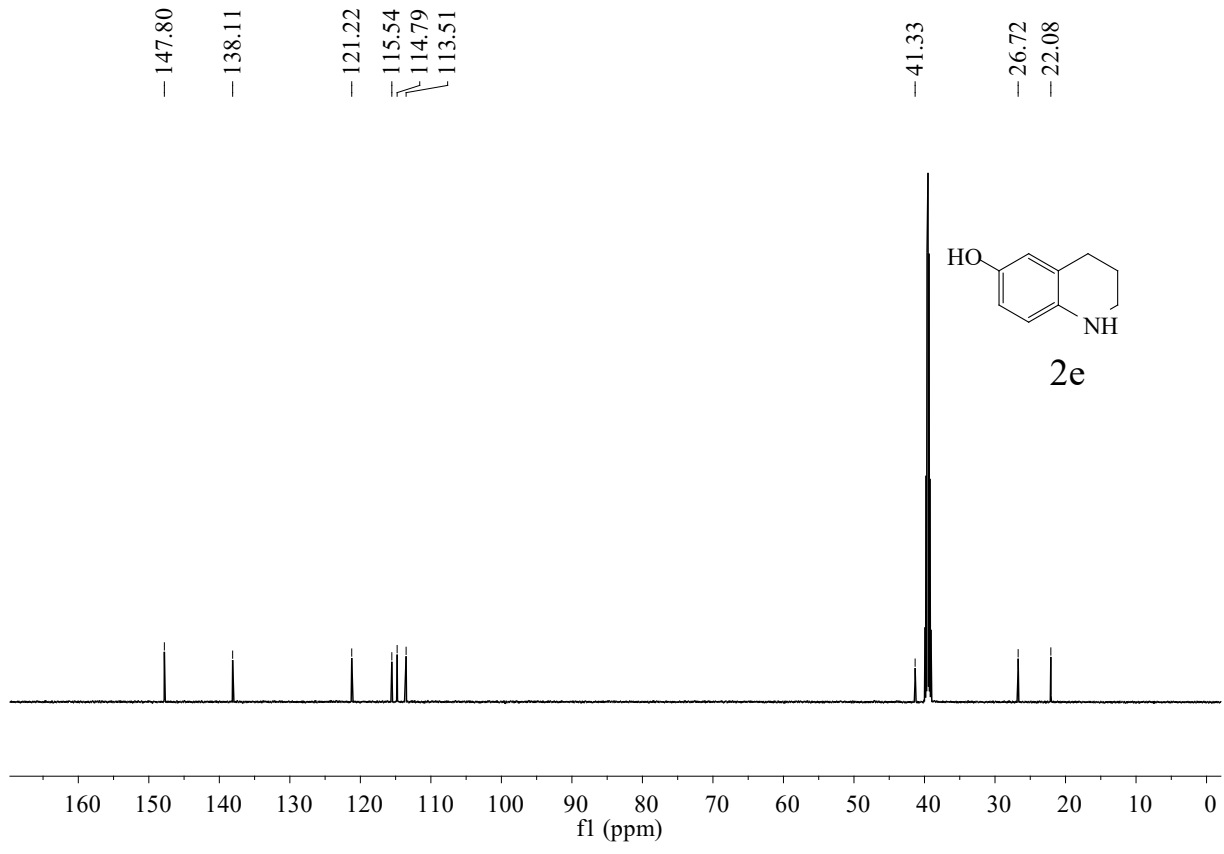
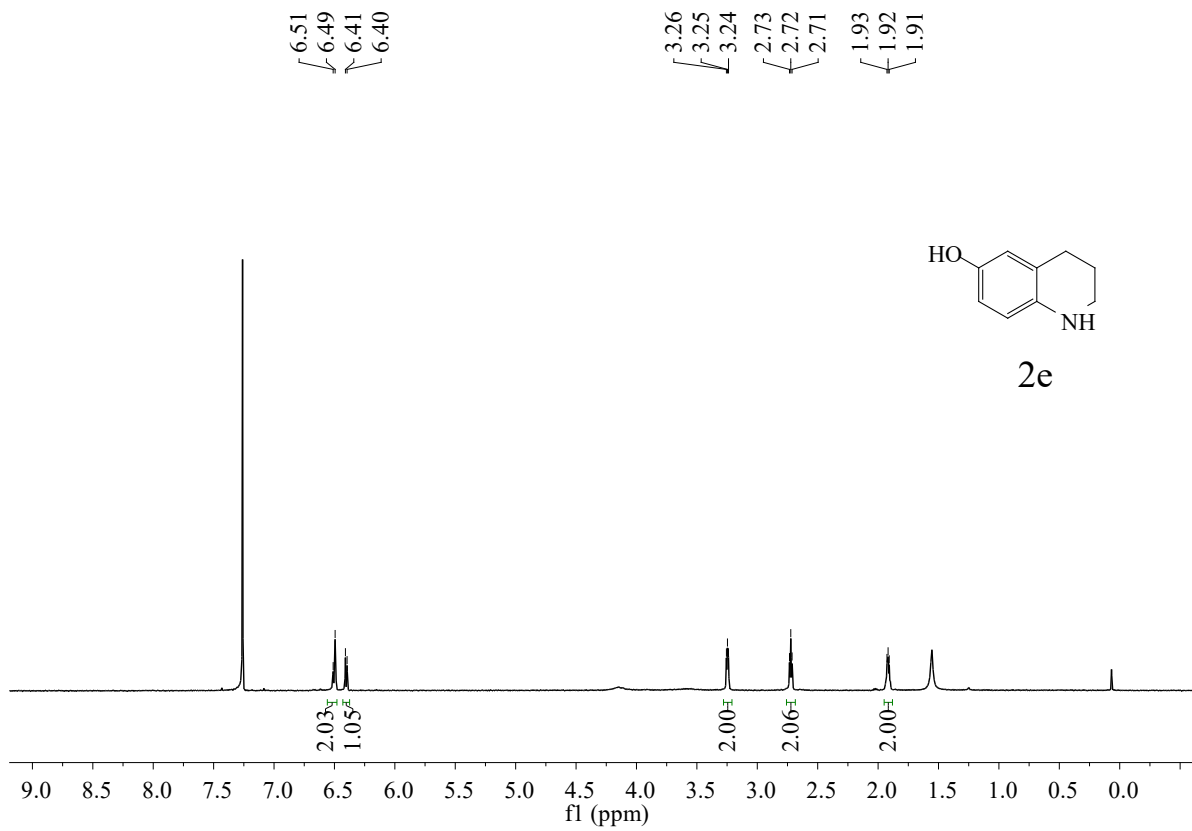


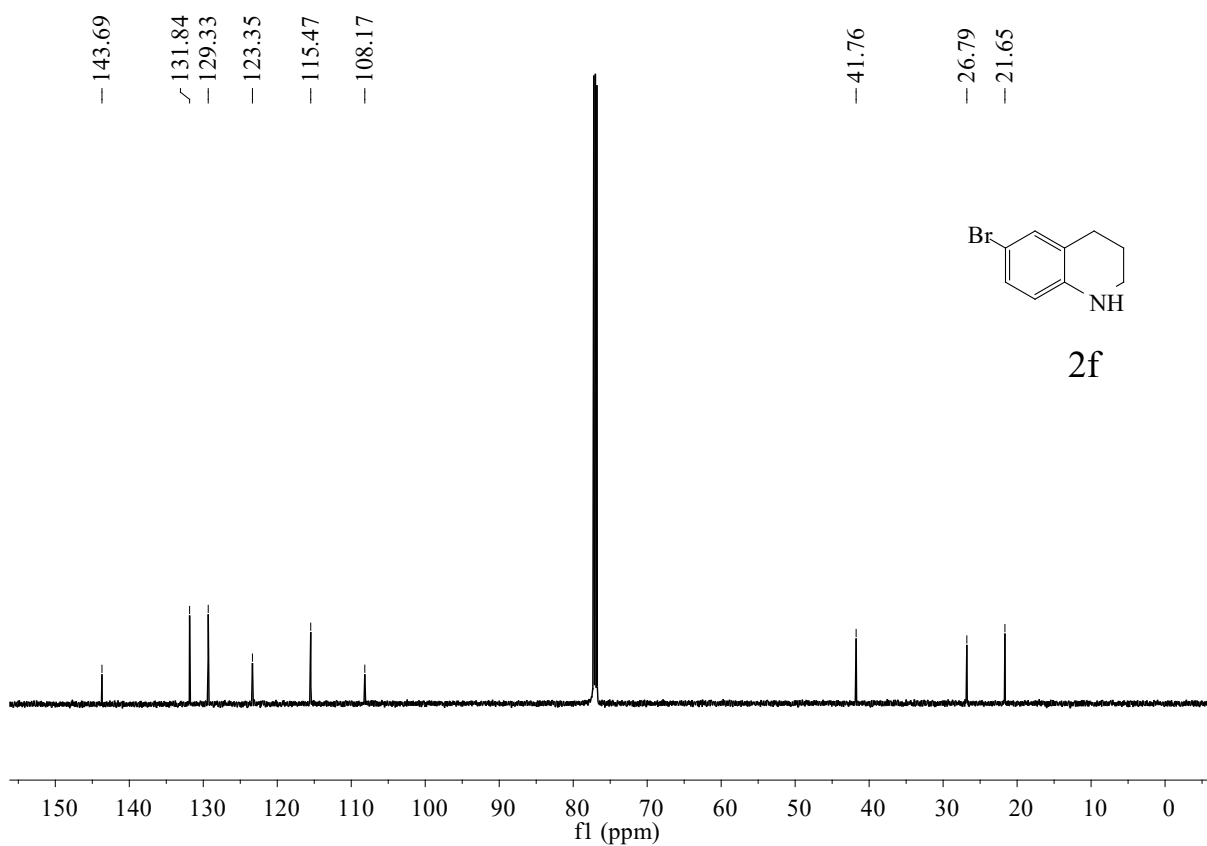
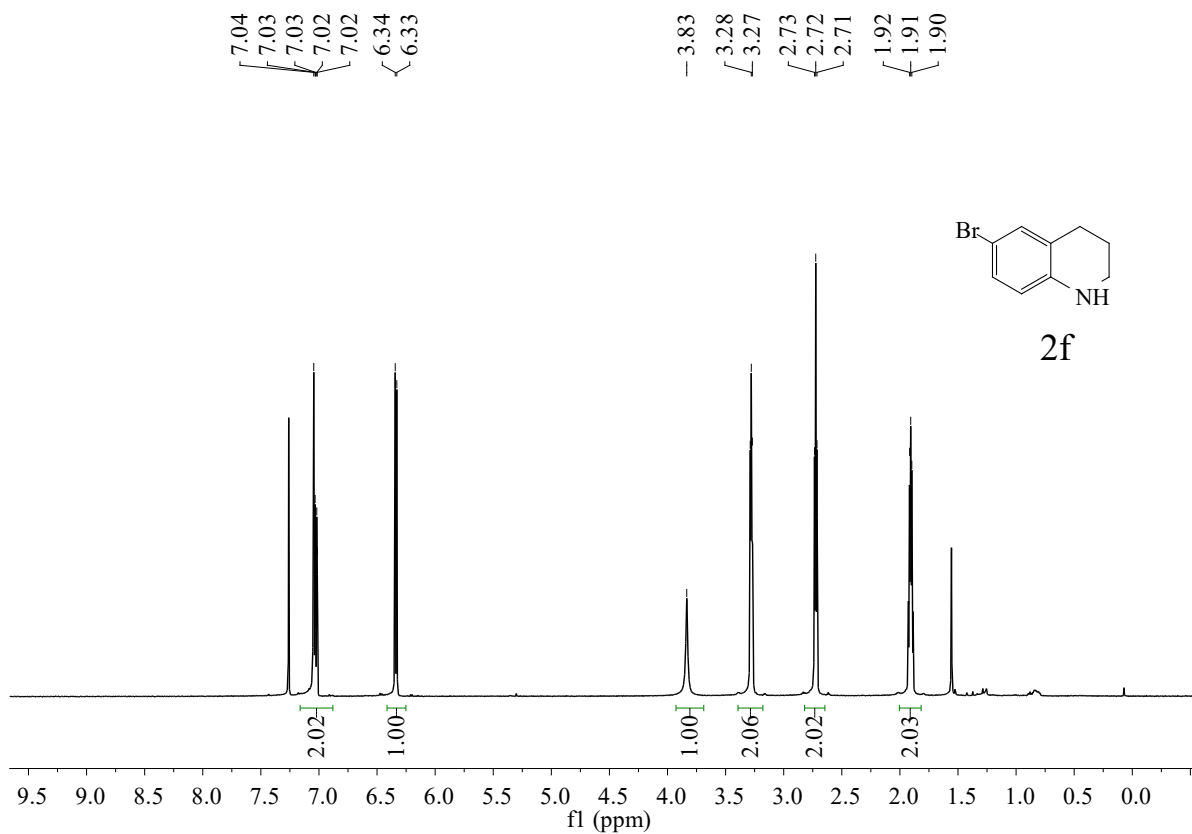


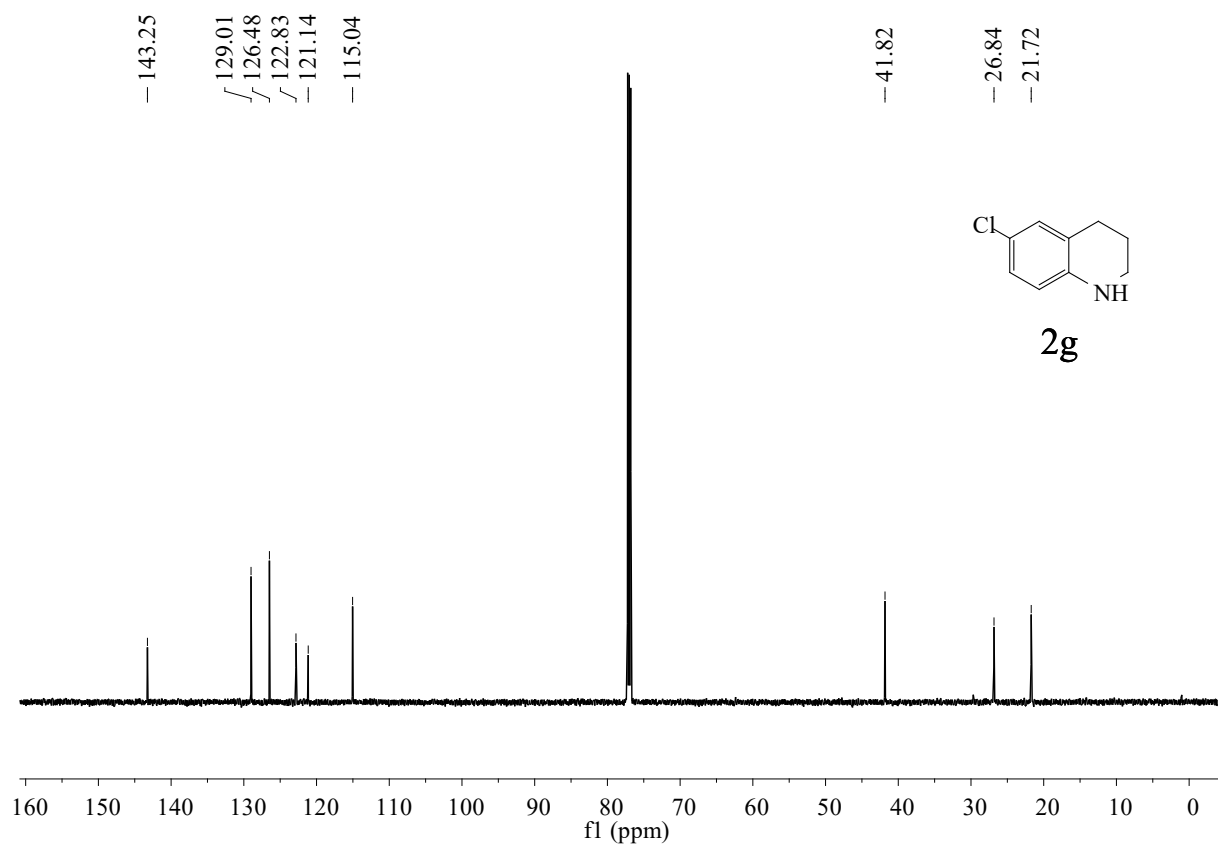
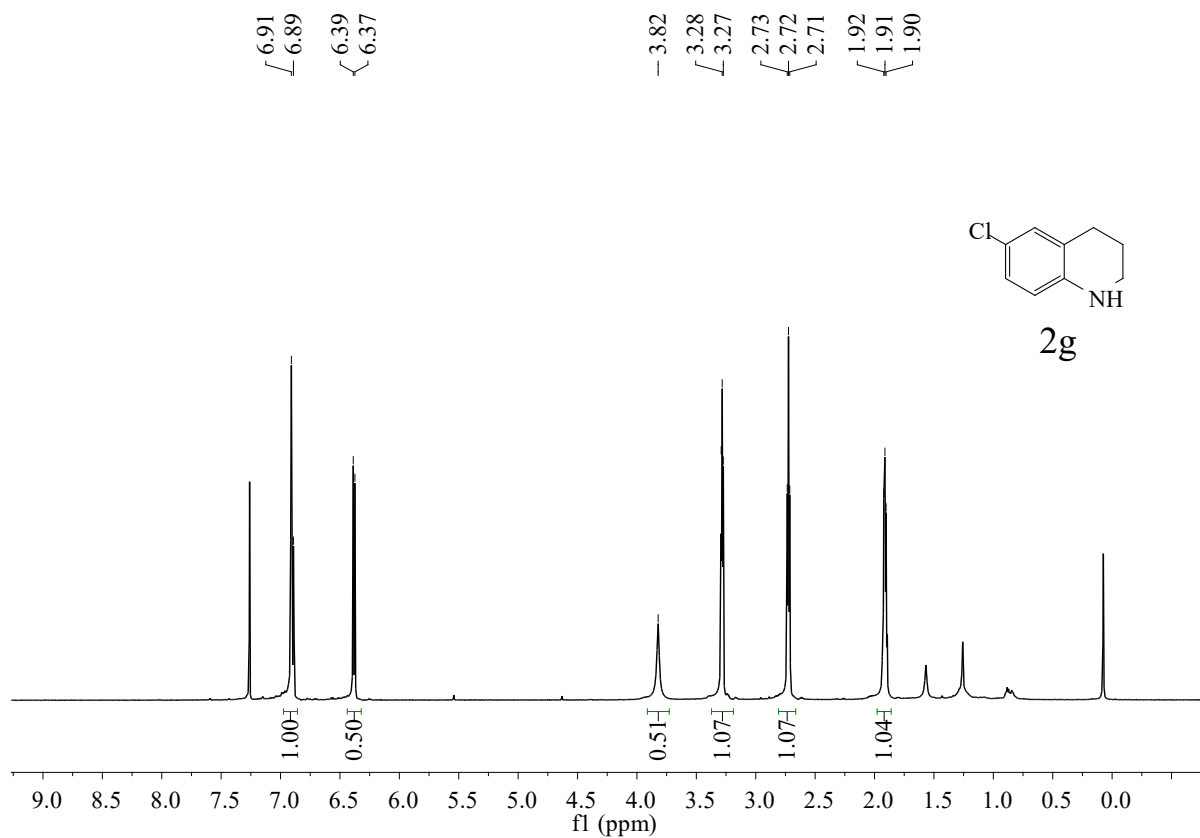


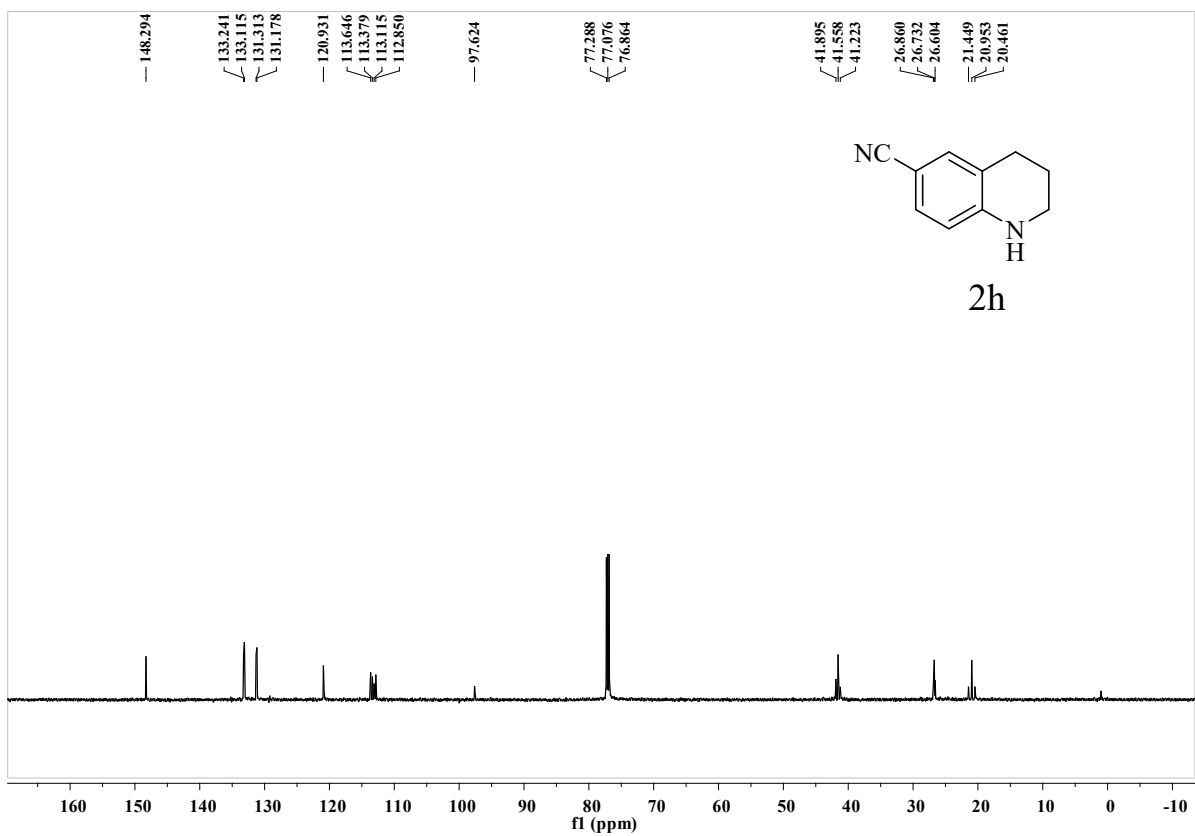
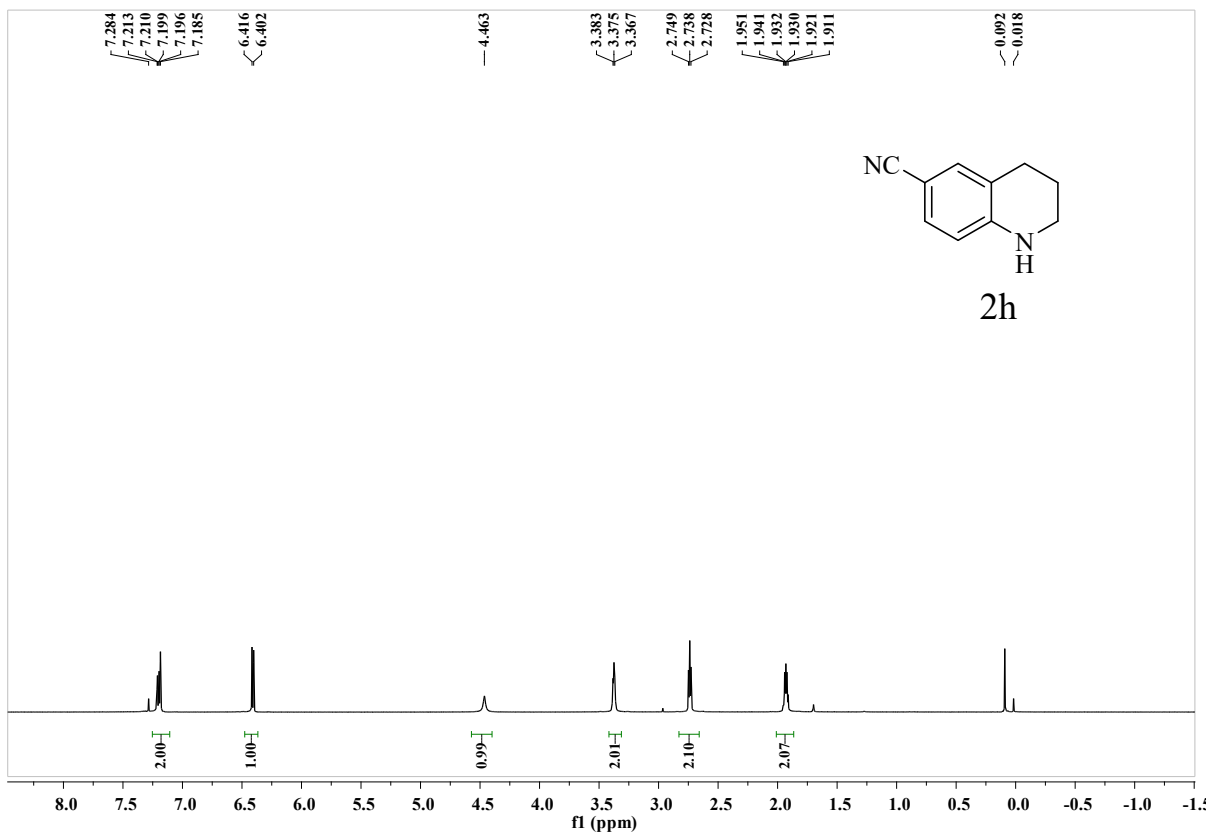


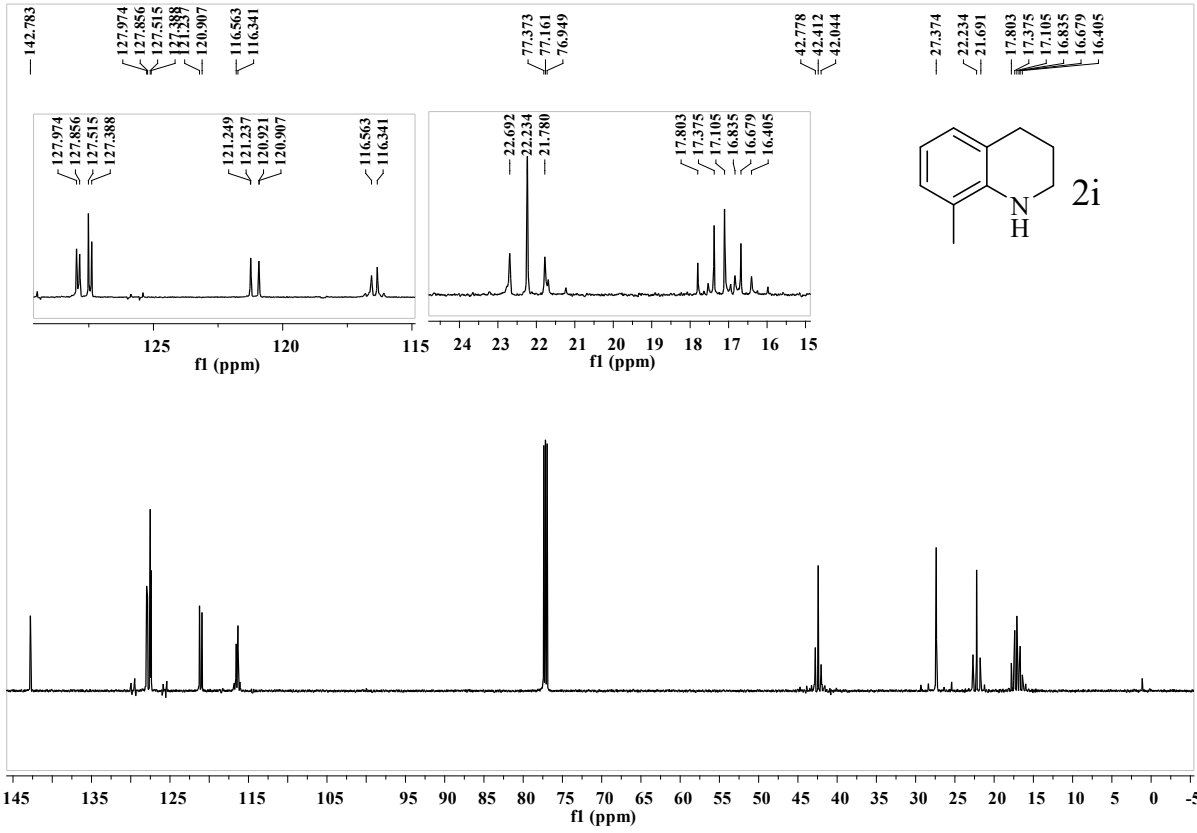
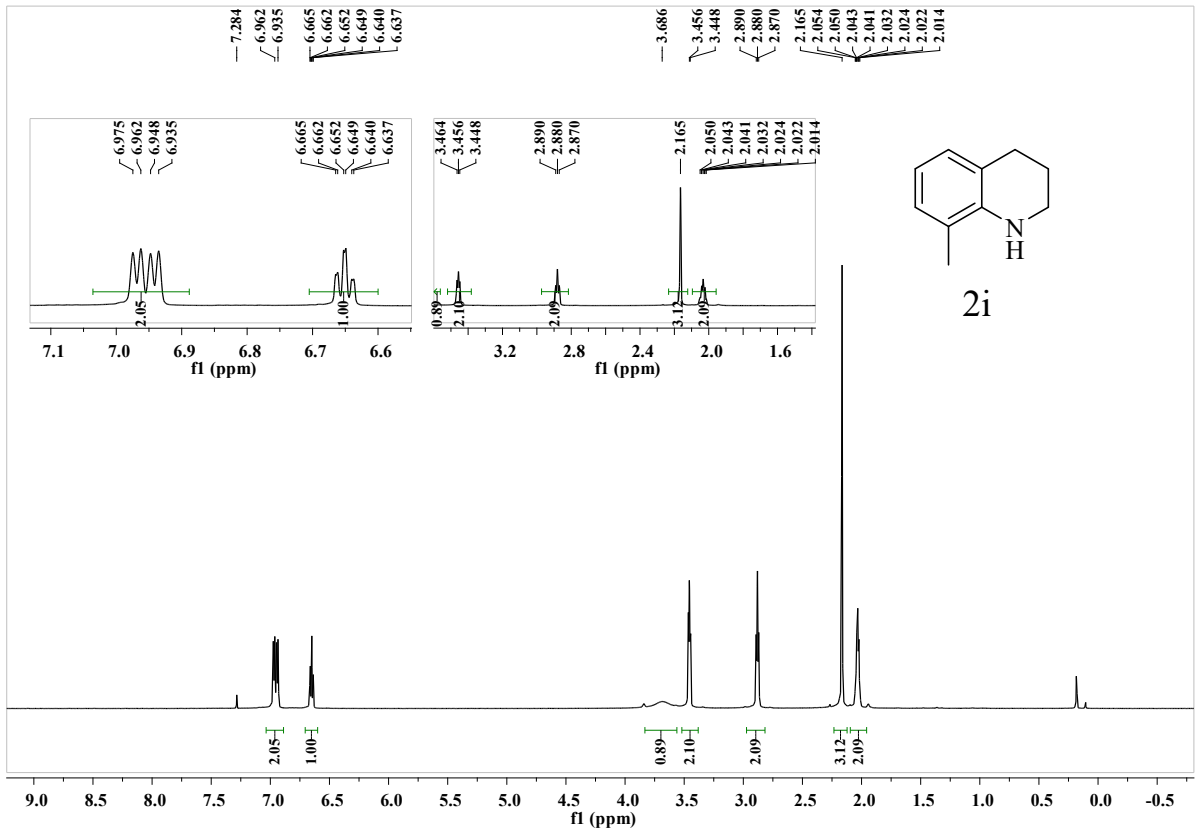


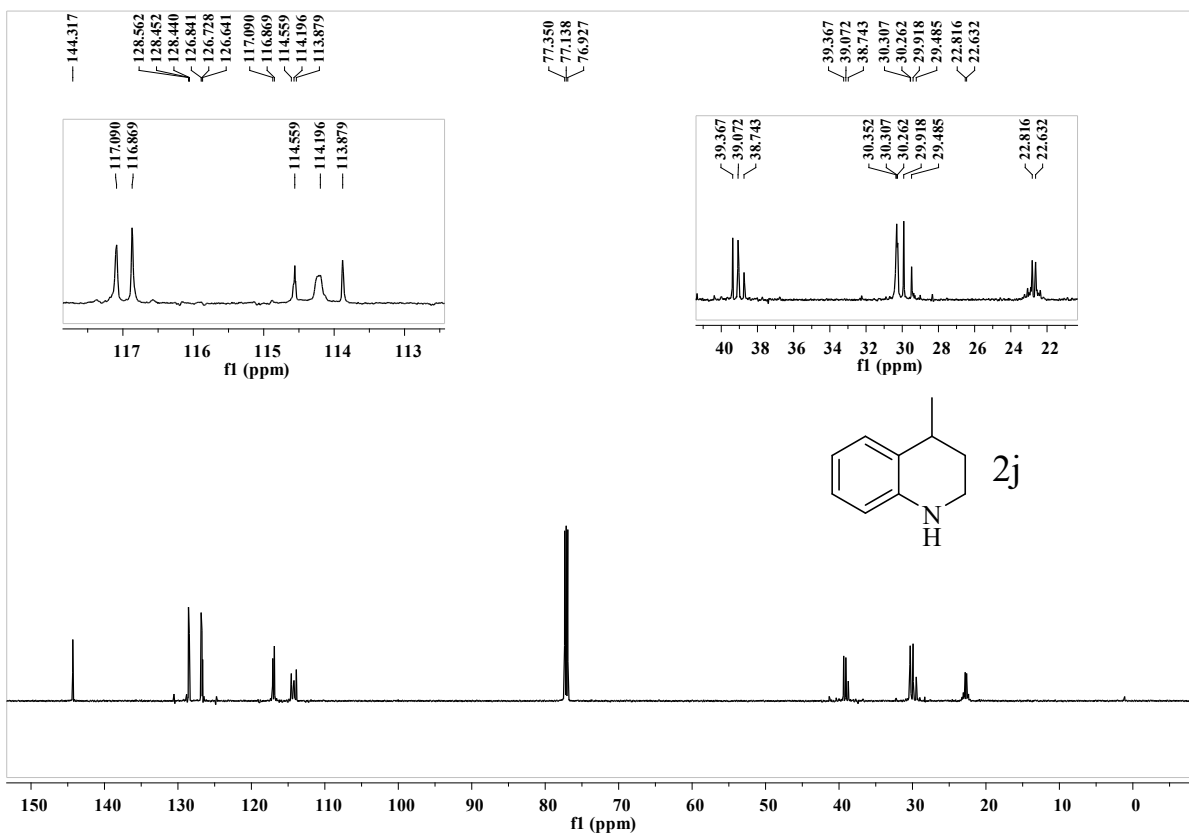
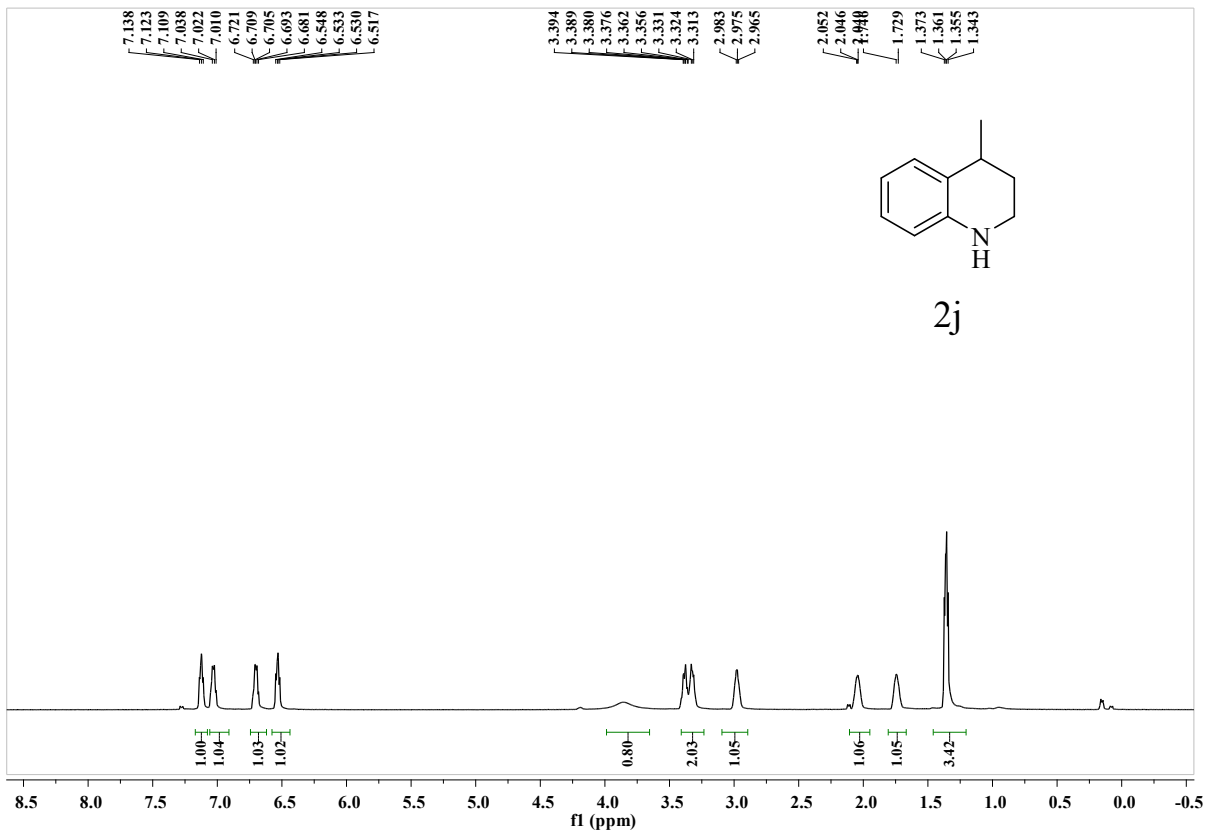


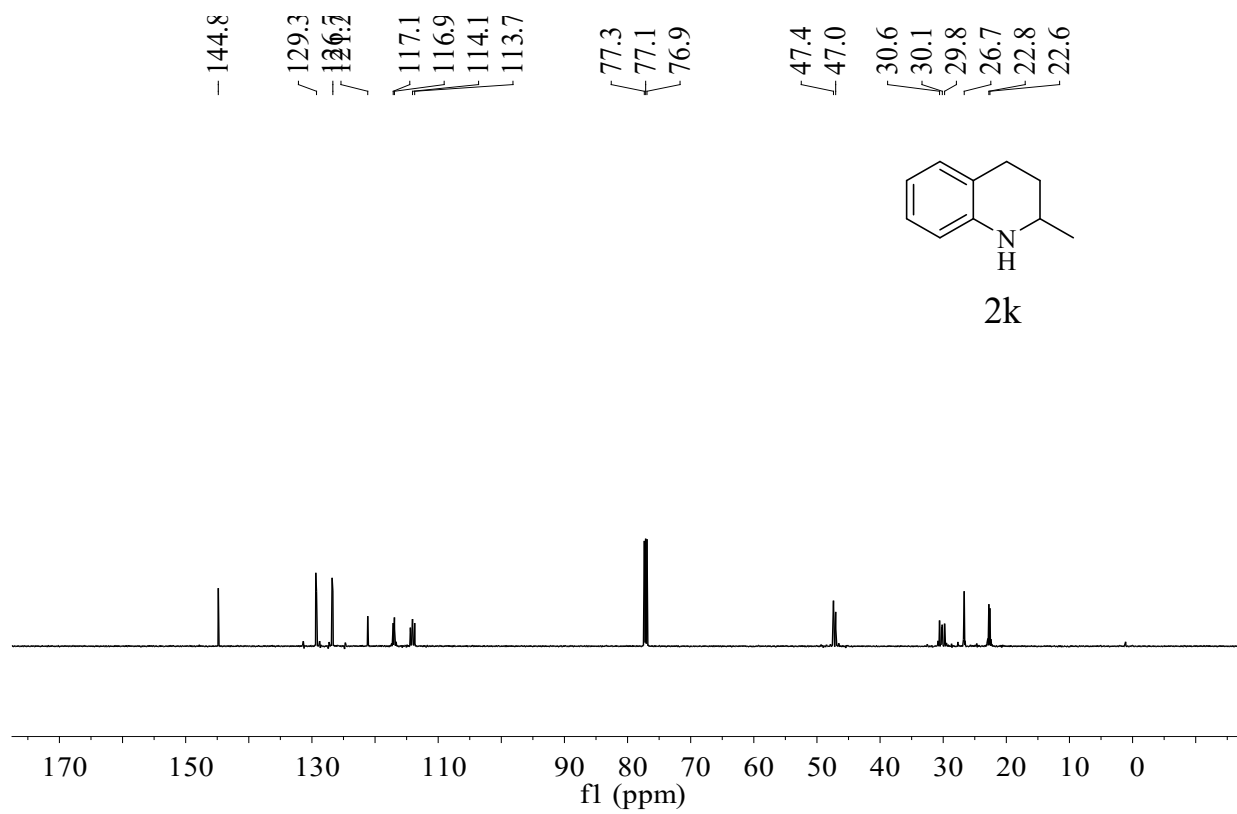
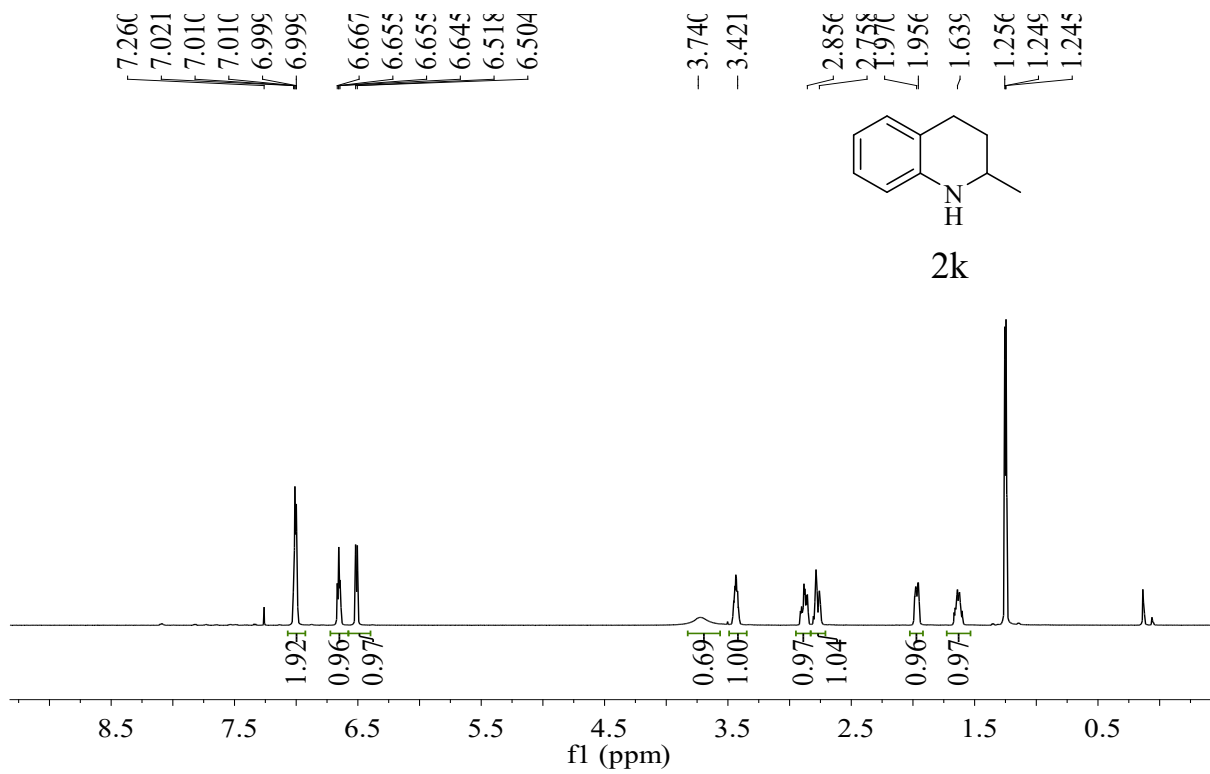


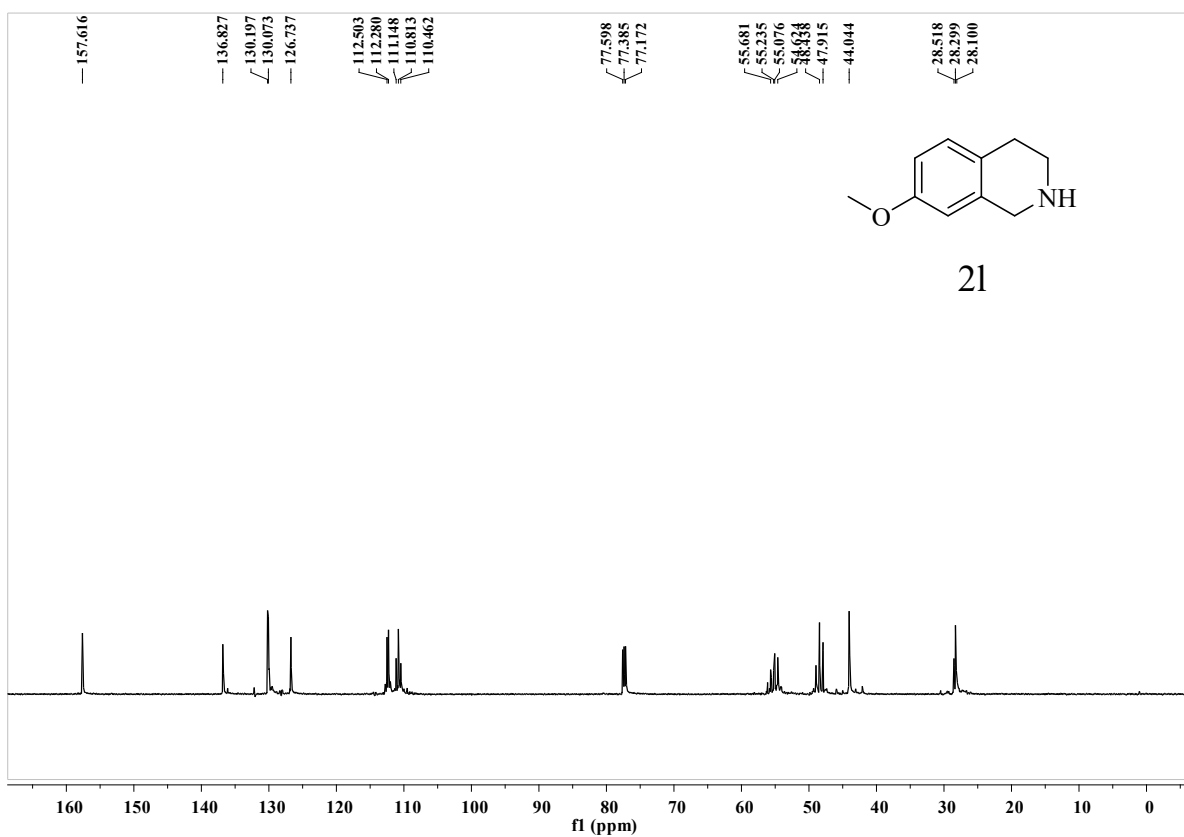
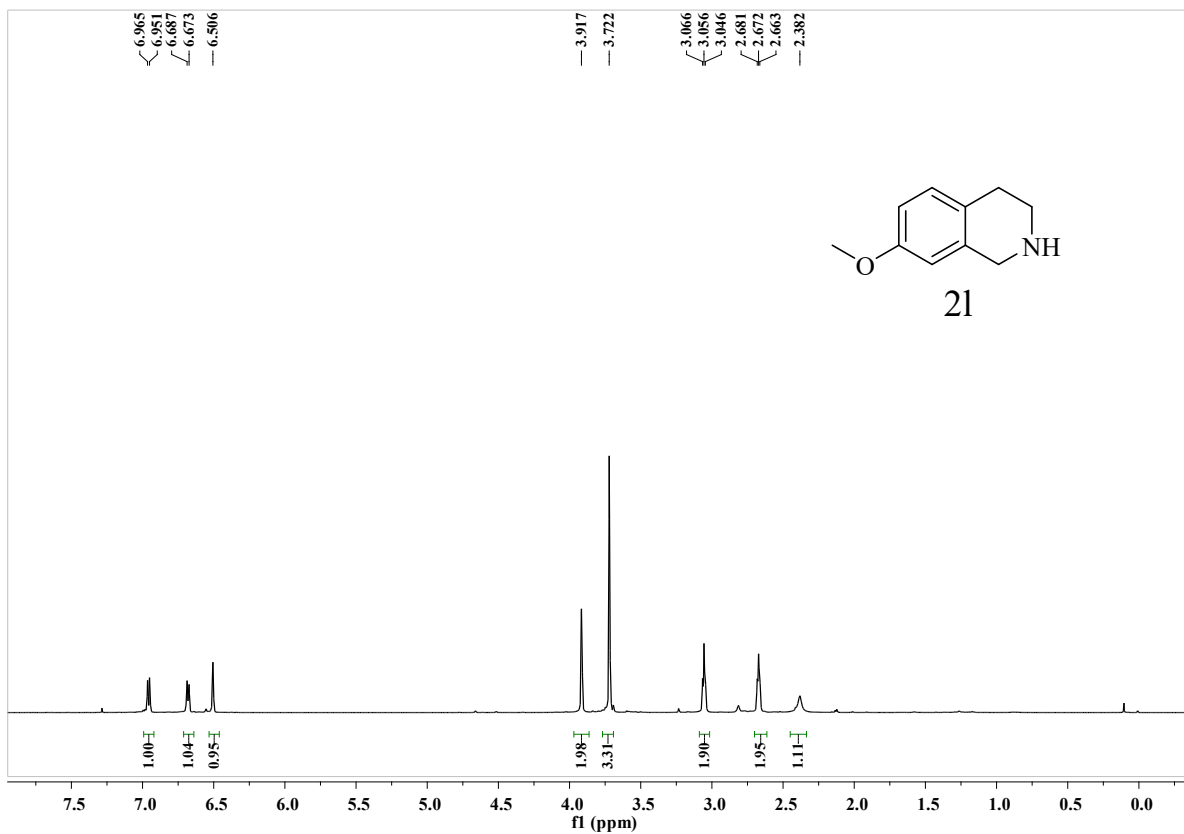


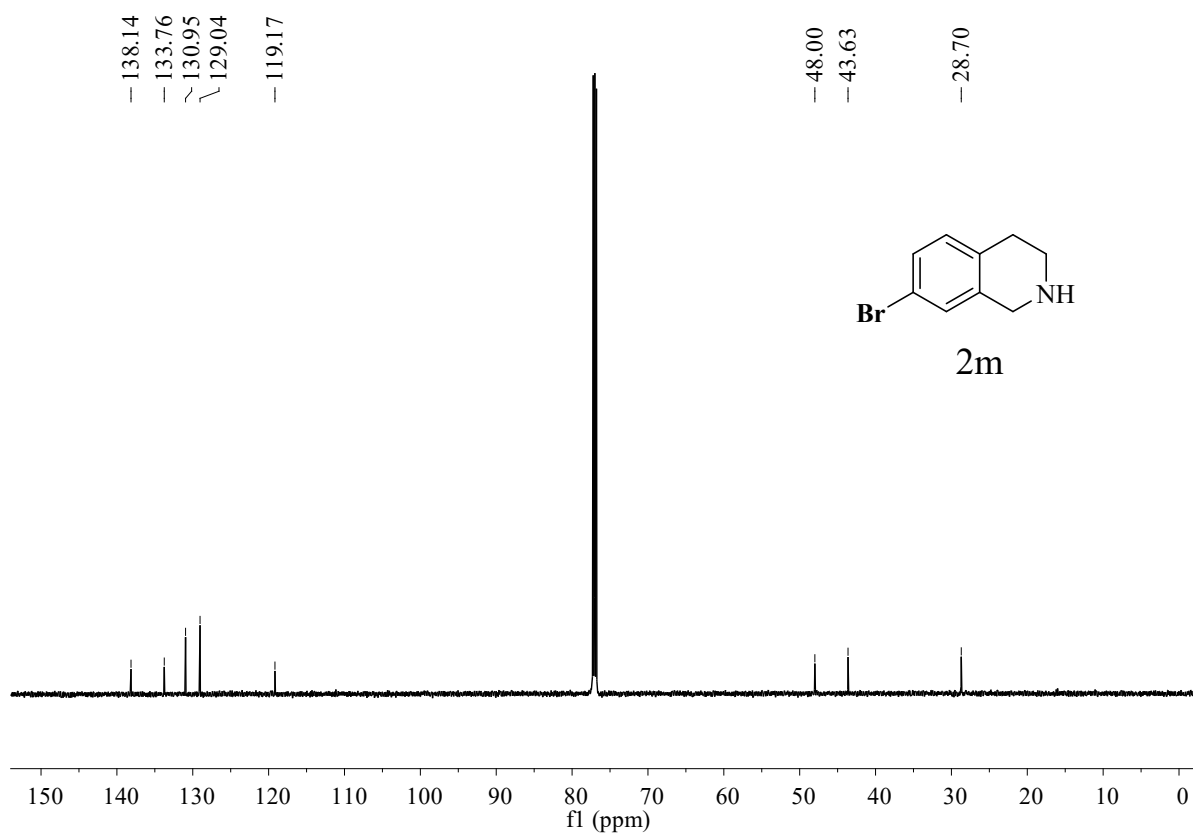
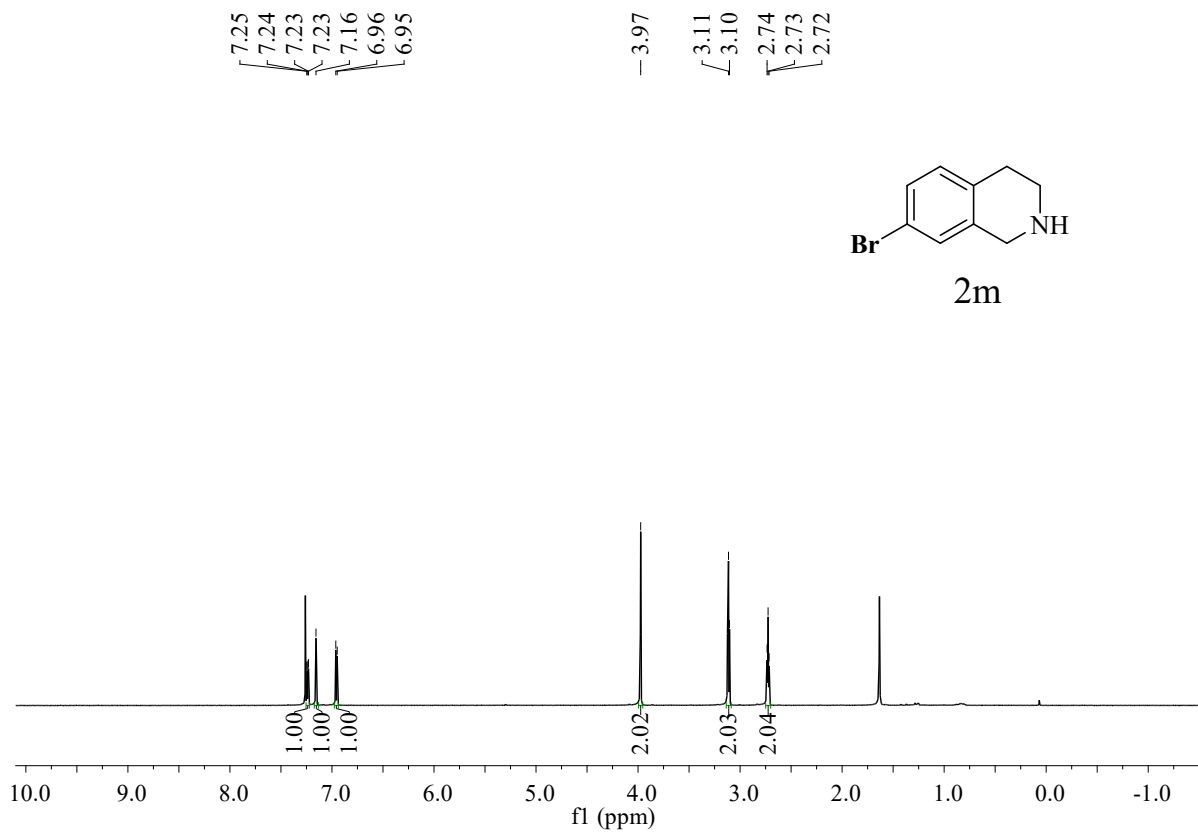


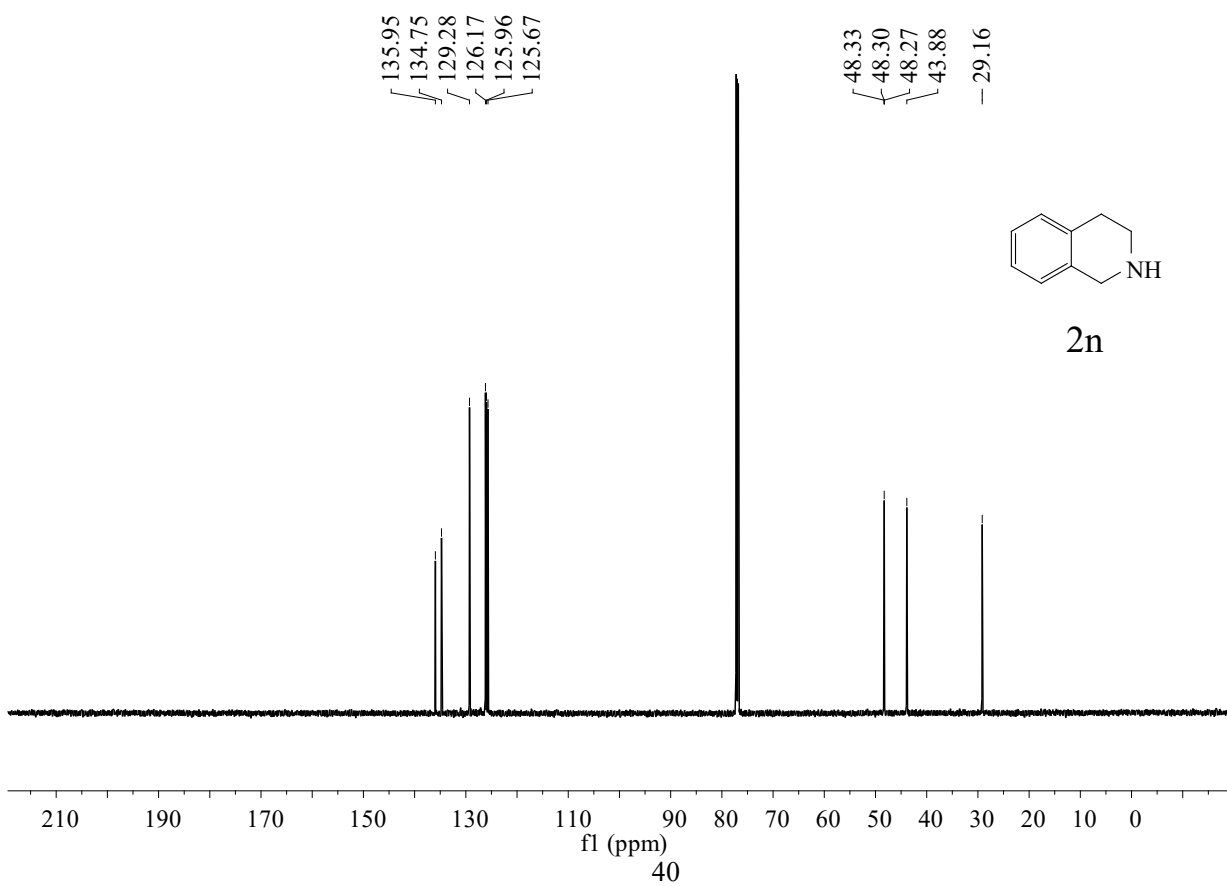
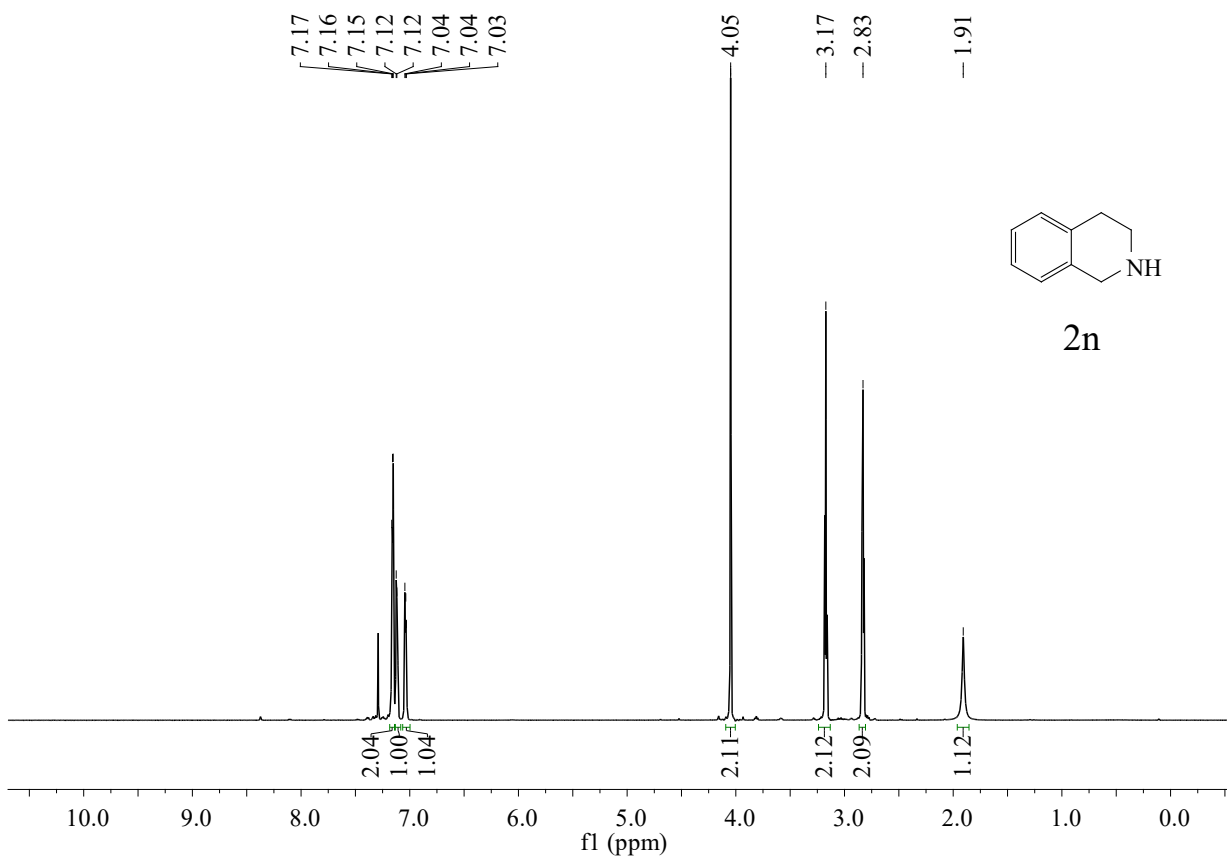


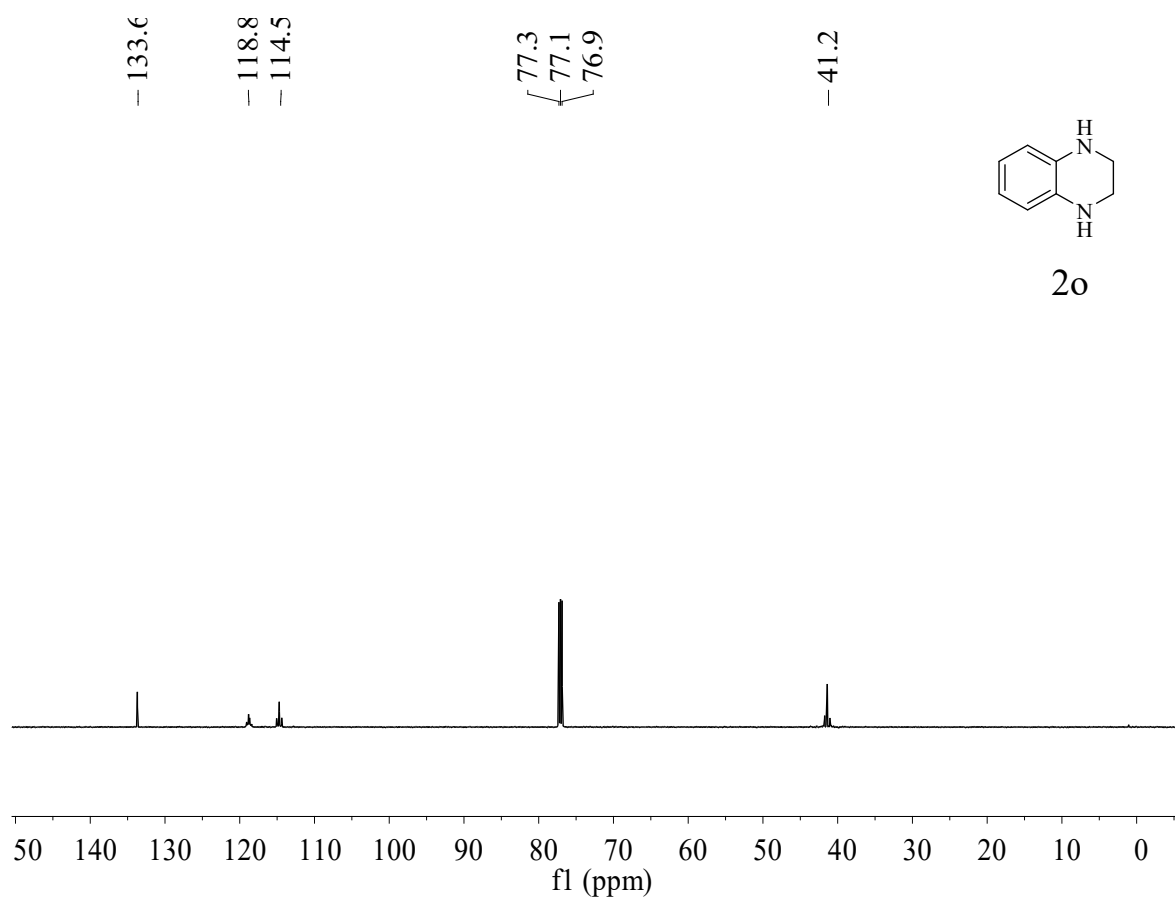
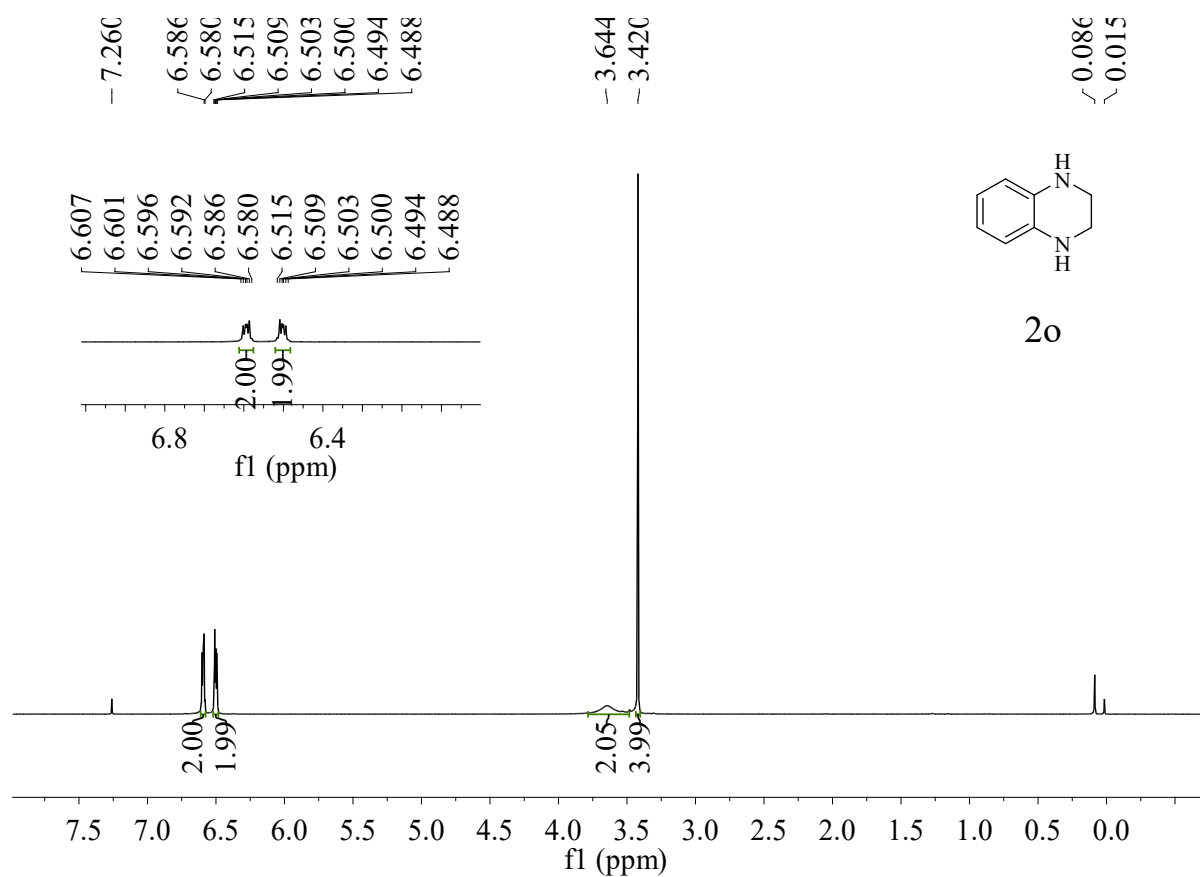












Section 7. References.

1. M. J. Frisch, G. W. Trucks, H. B. Schlegel, G. E. Scuseria, M. A. Robb, J. R. Cheeseman, G. Scalmani, V. Barone, G. A. Petersson, H. Nakatsuji, X. Li, M. Caricato, A. V. Marenich, J. Bloino, B. G. Janesko, R. Gomperts, B. Mennucci, H. P. Hratchian, J. V. Ortiz, A. F. Izmaylov, J. L. Sonnenberg, D. Williams-Young, F. Ding, F. Lipparini, F. Egidi, J. Goings, B. Peng, A. Petrone, T. Henderson, D. Ranasinghe, V. G. Zakrzewski, J. Gao, N. Rega, G. Zheng, W. Liang, M. Hada, M. Ehara, K. Toyota, R. Fukuda, J. Hasegawa, M. Ishida, T. Nakajima, Y. Honda, O. Kitao, H. Nakai, T. Vreven, K. Throssell, J. A. Montgomery, J. E. Jr. Peralta, F. Ogliaro, M. J. Bearpark, J. J. Heyd, E. N. Brothers, K. N. Kudin, V. N. Staroverov, T. A. Keith, R. Kobayashi, J. Normand, K. Raghavachari, A. P. Rendell, J. C. Burant, S. S. Iyengar, J. Tomasi, M. Cossi, J. M. Millam, M. Klene, C. Adamo, R. Cammi, J. W. Ochterski, R. L. Martin, K. Morokuma, O. Farkas, J. B. Foresman, D. J. Fox, Gaussian 16, revision B.01; Gaussian, Inc.: Wallingford, CT, 2016.
2. a) A. D. Becke, *J. Chem. Phys.* **1997**, *107*, 8554; b) A. D. Becke, *J. Chem. Phys.* **1993**, *98*, 5648; c) C. Lee, W. Yang, G. Parr, *Phys. Rev. B.* **1988**, *37*, 785.
3. a) R. S. Crees, M. L. Cole, L. R. Hanton, C. J. Sumby, *Inorg. Chem.* **2010**, *49*, 1712; b) Q.-J. Wu, M.-J. Mao, J.-X. Chen, Y.-B. Huang and R. Cao, *Catal. Sci. Technol.*, **2020**, *10*, 8026;
4. V. Jurkauskas, J. P. Sadighi, S. L. Buchwald, *Org. Lett.* **2003**, *5*, 2417;
5. Feng, D. W.; Gu, Z. Y.; Li, J.-R.; Jiang, H.-L.; Wei, Z.; Zhou, H.-C. Zirconium-metalloporphyrin PCN-222: mesoporous metal-organic frameworks with ultrahigh stability as biomimetic catalysts. *Angew. Chem. Int. Ed.* **2012**, *51*, 10307–10310;
6. Zhang, L. J.; Yuan, J. C.; Ma, L. J.; Tang, Z. Y.; Zhang, X. M. Selective hydroboration of alkynes via multisite synergistic catalysis by PCN-222(Cu). *J. Catal.* **2021**, *401*, 63–69;
7. a) L. Z. Bai, J. Y. Zheng, L. J. Ma, J. C. Yuan, X. Y. Song, J. Y. Lu, L. J. Zhang, X.-M. Zhang, Donor–Acceptor-Conjugated Porous Polymer for Photopromoted N–H Formylation of Secondary Amines: Efficient In Situ N-Heterocyclic Carbene Catalysis in Radical Manner. *ACS Catal.* **2024**, *14*, 3889–3899; b) X. Y. Song, Q. Gao, N. Zhang, L. J. Zhang, J. Y. Lu, J. C. Yuan and X.-M. Zhang, Metalation of porphyrin to polarize electric field of conjugated porous polymers: Efficient photooxidation for Csp²–O radical cross-coupling reaction assisted by hydrogen bonds, *ACS Appl. Mater. Inter.*, **2025**, *17*, 43070–43079.
8. Z.-H. He, N. Li, K. Wang, W.-T. Wang, Z.-T. Liu. Selective hydrogenation of quinolines over a CoCu bimetallic catalyst at low temperature. *Molecular Catal.*, 2019, **470**, 120–126;
9. W. M. Chen, Z. Yao, W. X. Chen, Q. K. Shen, D. S. Yuan, C. Zhang, Y. F. Zhu, H.-W. Liang, Y.-G. Wang, W. G. Song, C. Y. Cao. Fully exposed iridium clusters enable efficient hydrogenation of N-heteroarenes. *ACS Catal.*, 2023, **13**, 12153–12162;
10. K. Wang, Z. Cao, J. L. Wang, Z.-H. He, D. Wang, R.-R. Zhang, W. T. Wang, Y. Yang, Z.-T. Liu. Efficient and selective hydrogenation of quinolines over Fenicu/MCM-41 catalyst at low temperature: Synergism of Fe-Ni and Ni-Cu alloys. *Molecular Catal.*, 2022, **520**, 112166;
11. A. Bathla, B. Pal. Bimetallic Cu(core)@Zn(shell) co-catalyst impregnated TiO₂ nanosheets (001 faceted) for the selective hydrogenation of quinoline under visible light irradiation. *J. Ind. Eng. Chem.*, 2019, **79**, 314–325;
12. Y. T. Gong, P. F. Zhang, X. Xu, Y. Li, H. R. Li, Y. Wang. A novel catalyst Pd@ompg-C₃N₄ for highly chemoselective hydrogenation of quinoline under mild conditions. *J. Catal.*, 2013, **297**, 272–280;
13. R. Rahi, M. F. Fang, A. Ahmed, Sánchez-Delgado, R. A. Hydrogenation of quinolines, alkenes, and biodiesel by palladium nanoparticles supported on magnesium oxide. *Dalton T.*, 2012, **41**, 14490;
14. a) W. H. Mao, D. G. Song, J. Y. Guo, K. L. Zhang, C. D. Zheng, J. Lin, L. Huang, L. Z. Zheng, W. H. Zhong and F. Ling, Manganese-catalyzed asymmetric transfer hydrogenation of quinolines in water using ammonia borane as a hydrogen source, *Green Chem.*, **2024**, *26*, 5933–5939; b) W. M. Chen, Z. Yao, W. X. Chen, Q. K. Shen, D. S. Yuan, C. Zhang, Y. F. Zhu, H.-W. Liang, Y.-G. Wang, W. G. Song and C. Y. Cao, Fully exposed Iridium clusters enable efficient

hydrogenation of N-heteroarenes, *ACS Catal.*, **2023**, *13*, 12153-12162; c) K. Wang, Z. Cao, J. L. Wang, Z.-H. He, D. Wang, R.-R. Zhang, W. T. Wang, Y. Yang and Z.-T. Liu, Efficient and selective hydrogenation of quinolines over FeNiCu/MCM-41 catalyst at low temperature: Synergism of Fe-Ni and Ni-Cu alloys, *Molecular Catal.*, **2022**, *520*, 112166.